EUROPEAN ORGANIZATION FOR NUCLEAR RESEARCH

CERN/SPSC/74-10
SPSC/P 5
January 24, 1974

PROPOSAL TO THE SPSC

MEASUREMENT OF BACKWARD 2-BODY AND QUASI-2-BODY REACTIONS INDUCED ON UNPOLARIZED AND POLARIZED PROTONS BY $\pi^{\pm}$, $K^{\pm}$, $\bar{p}$ RANGING FROM 25 TO 120 GeV/c

R. Barate, P. Bareyre, P. Bonamy, P. Borgeaud, J.C. Brisson,
M. David, J. Ernwein, J. Feltesse, G. Laurens, P. Le Du,
Y. Lemoigne, H. Roussarie, A. Roussarie, G. Villet,

Département de Physique des Particules Elémentaires, CEN-Saclay, France.

B. Brabson, M. Corcoran, R. Crittenden,
R. Heinz, H. Neal, D. Rust,

Indiana University, Bloomington.

Jan. 14 th 1974.

ABSTRACT :

We propose to measure, in the 20 - 120 GeV/c range, two body and quasi-two body baryon exchange reactions for $|u| \leqslant 1$ $(GeV/c)^2$. The experimental apparatus consists of two spectrometers which determine the angles and momenta of the forward and backward outgoing particles. The detectors cover a large solid angle : 3 msr for the forward arm and 3 sr for the backward arm. They are designed to operate at incident beam rates of 1.0×10^7 particles/pulse and will measure cross sections down to the nb/$(GeV/c)^2$ range.

PHYSICS INTEREST

In a simple billiard ball picture of πp backward elastic scattering, the π will strike the proton "head-on", thereby undergoing a large acceleration with, in general, the attendant radiation of hadronic matter. In a statistical analysis of this interaction, elastic scattering (no radiation) has to compete with other final states, resulting in a backward elastic cross section that will drop as a power law of s for fixed u. In this elegant yet simple picture of the interaction, a knowledge of the value of the power and its u dependence would be very interesting [1,2].

If hadronic matter contains parton seeds, backward πp scattering at high energies could be dominated by parton-parton scattering. This could lead to a break in the s-dependence of $d\sigma/d$, the break occurring where the dominant mechanism for the reaction changes. For example, Regge exchange might be primarily responsible for the reaction at lower s, $s \lesssim 80$ GeV^2($P_{lab} \lesssim 40$ GeV/c), and parton-parton interactions, which presumably would fall more slowly with s, would then take over primary responsibility for backward πp scattering. This would most likely occur at large (-u), say $u=-1.(GeV/c)^2$, where conventional baryon exchange amplitudes are low.

Since the birth of Regge theory about ten years ago, backward πp elastic scattering has been interpreted as arising from the exchange of baryon Regge trajectories in the u-channel. More recently, attempts have been made to improve this model by adding Regge cuts to the Regge poles [3]. Our data will make direct tests of important Regge predictions.

In a Regge model the cross section can be written as:

$$\frac{d\sigma}{du} = A(u)\, s^{\cdot\, 2\alpha_{eff}^{(u)} - 2}$$

where α_{eff} is the leading Regge trajectory in the Regge pole model, and is the effective trajectory in the Regge cut model. As s in-

This "shrinkage" has not been observed below 20 GeV/c in backward $\pi^- p$ scattering, a particularly simple reaction from the Regge viewpoint since there is presumably just one leading trajectory (A_δ). If we observe no shrinkage in $\pi^- p$, the Regge pole model would be ruled out[3]. A particularly exciting aspect of backward $\pi^+ p$ scattering is the existence of a prominent dip at $u \approx -.2$ $(GeV/c)^2$. [4]. This dip occurs just where the leading trajectory (N_α) passes through a wrong signature nonsense point ($\alpha = -\frac{1}{2}$). Originally this dip was considered a triumph for the Regge pole model, although subsequently this structure was interpreted as due to an interference between the pole and the cut amplitudes. Already at 20 GeV/c a measurement of the dip will have a significant influence on the destiny of Regge models [3]. The various Regge exchange models make similarly different predictions for the high s behaviour of $\frac{d\sigma}{du}$ away from 180°. For example at 50 GeV/c and $u = -1 (GeV/c)^2$, the predictions vary by an order of magnitude and these predictions are insensitive to the parameters in the models [3]. Quoting from the review paper of Berger and Fox [3] on Regge models for backward $(0 \lesssim -u \lesssim 1 (GeV/c)^2)$ πp scattering, "studies at 30 to 70 GeV/c should be immensely valuable".

The optical model, although usually associated with forward scattering, is intimately concerned with scattering at all angles - in particular, backward scattering. For example, Chu and Hendry show how the dip in backward $\pi^+ p$ scattering at $u \simeq -.2 (GeV/c)^2$ can be associated with a peripheral interaction whose contribution in the backward direction goes essentially as $J_o(R\sqrt{-u})$, where J_o is the usual Bessel function.[5]. A major drawback to the optical model has been its lack of built-in energy dependence. However, instead of summing contributions from different impact parameters one can use a closed form for an s-channel Regge pole, resulting in an optical model containing energy dependence. Work on this modified optical model is in progress [6], and our proposed experiment should provide a stringent test of the model, assuming it is different from the u-channel Regge pole prediction.

To our knowledge, there exists no data for backward πp elastic scattering at 20 GeV/c and above. Cross sections and especially pola-

EXPERIMENTAL ARRANGEMENT

Beam

We propose to do the experiment in beam H_1 (or $E1_2$*). The beam intensity we require is 10^7 particles/burst, which is possible for both beam polarities for momenta between 25 and 120 GeV/c with a momentum bite of ($\pm$ .4 %) [9]. We require two DISC Cerenkov counters and one threshold Cerenkov in the beam. The threshold counter would be set to detect π's and would be used in the trigger in coincidence, One DISC counter would be for K's, in coincidence in the trigger. The other DISC, set for p's and $\bar{p}$'s, would be in anticoincidence for p's and in coincidence for $\bar{p}$'s.

Two hodoscopes H_0 and H_1 measure the incoming pion direction. They are shown in Figure 1. They are located 17. m and 2.35 m upstream of the center of the magnet "Goliath" which analyses the backward scattered pion. H_0 (4.0 x 4.0) cm^2 and H_1 (1.1 x 1.1) cm^2 both have logical units 1 mm wide.

Target

A liquid hydrogen target 1.5 m long and 3 cm in diameter is located inside the magnet "Goliath". The vacuum tank is made of aluminum 1 mm thick.

Forward Spectrometer

The forward proton is analysed in a magnetic spectrometer. (See Fig. 1). The magnet "Mimosa", supplied by Saclay, is a C-magnet 20 cm high x 40 cm wide x 240 cm long with a bending power of 3.12 Tesla-meters. We will move Mimosa in order to match the forward spectrometer solid angle and momentum resolution to the needs of the

---

* $E1_2$, although limited to 80 GeV/c, has the interesting possibility of providing a high flux of electrons. Our spectrometer completed with an electron detector could be well suited for some electroproduction measurements.

experiment, as shown in the following table :

Beam Momentum (GeV/c)	Mimosa Magnetic Field (KGauss)	Goliath-Mimosa Separation, Center-to-Center (m)	Mimosa Solid Angle (msr)	Forward Momentum Resolution (%)	Forward Angular Resolution (mr)
25.	13.	3.9	2.7	.9	.50
40.	13.	3.9	2.7	I.3	.25
75.	13.	7.I	I.I	I.5	.21
120.	13.	11.2	0.5	I.7	.15

Figure 1 shows Mimosa in the 75 GeV/c position.

To deal with the high flux, two scintillator hodoscopes H_2 (8.0 × 6.0) cm^2 and H_3 (25.0 cm wide × 12.0 cm high) serve as detectors for the upstream lever arm. Note that both hodoscopes have a ±.5mm resolution. At 25 GeV/c they are located at I.20 m and 2.2m from the Goliath center respectively. H_2 is stationary and H_3 is attached to Mimosa and moves with it. In order to avoid the use of too many phototubes, those hodoscopes will overlap.

In connexion with Prof. Charpak we have started tests on a small MWPC (5 × 5 cm) with a spacing of 0.5 mm between the read-out wires (diameter = 5 μm). If it is verified that these chambers can tolerate the expected fluxes, having a time resolution approaching 10 nsec, we shall use them for the H_2 and H_3 hodoscopes.

The downstream lever arm is made up of two proportional wire chambers PC1 (50 cm wide x 22 cm high) and PC2 (90 cm wide x 40 cm high). They both have 1 mm wire spacing. C4 is a scintillator located just downstream of PC2. Two Cerenkov counters TC 1 and TC 2 are needed to reject the fast mesons at 75 GeV/c. TC1 is 4 m long and located upstream of Mimosa magnet and should have an inefficiency of 5.10^{-3} at 75 GeV. TC2 is 8 m long and placed between the proportional chambers PC 1 and PC 2. Its inefficiency should be of the order of 5.10^{-4}. Between 25 and 40 GeV/c only TC 1 is used, and it is located in the TC 2 position shown in Fig. 1. From 40 to 60 GeV/c, only TC2 is used. At 75 GeV/c or less, the global inefficiency is better than 10^{-7} and is sufficient to reject the fast forward mesons, which are of the order of 10^5 times more numerous than the protons. TC1 and TC2 can work for an incident momentum ranging from 20 to 120 GeV/c when filled with appropriate gas mixtures near atmospheric pressure. Further details on the Cerenkov counters efficiencies are given in Appendix 1.

The momentum acceptance of the forward spectrometer is $\geqslant 0.5P_i$ where P_i is the beam momentum. We plan to reduce this bite to $\geqslant 0.75P_i$ by using information from H3, PCI, and PC2 in the trigger. We compute on line the distance "D" between the impact in H3 and the intersection of the line defined by the impacts in PCI and PC2 with the H3 plane. The forward protons from elastic scattering have a "D" value lower than most other forward protons from inelastic reactions. This will reduce the trigger rate from low momentum p's and also from low momentum K's for which the TC1 and TC2 efficiencies will be low.

Backward Spectrometer

This spectrometer is of the non-focusing type and is capable of making a momentum analysis in the range of 0.3 GeV/c to 1.3 GeV/c for particles emitted between 75° and 180° in the laboratory. The solid angle subtended is of the order of 3 steradians.

The momentum dispersion is provided by the large magnet

To look at the backward meson trajectory we use 14 proportional wire chamber modules distributed on each side of the target and spaced 12 cm apart. Each module (1.8 m x 0.8 m useful area) consists of three planes of active wires 2 mm apart, the first being horizontal, the second vertical, and the third inclined at 15° with respect to the horizontal plane. All the modules are mechanically standard, but only the wires which lie in the useful solid angle are equipped with electronics. A fast output pulse from the second chambers on each side of the target will be used in the trigger.

The backward spectrometer has a momentum resolution of and an angular resolution which are independent of the beam mome... Their valuesare given in the following table.

u Range $(GeV/c)^2$	Momentum Resolution (%)	Angular Resolution (mr)
$0 \rightarrow -.4$	1.5	8
$-.4 \rightarrow -.8$	2.0	7
$-.8 \rightarrow -1.2$	2.5	7

TRIGGER, YIELD, BACKGROUND

The trigger requires at least one charged particle in each spectrometer and none outside the solid angle covered by the wire chambers. This condition is fulfilled when :

- the beam (H_0 H_1) is in coincidence with a forward scattered particle (H_2 H_3 C_4) and a backward scattered particle (fast OR pulse of the proportional chambers closest to the target) ;

- no veto comes from the anticoincidence counters AC1, AC2, AC3 (see Fig. 1) ; those counters are sensitive to neutral and charged particles ;

- no fast particle is detected by the two forward Cerenkov counters TC1 and TC2.

- a forward positive particle with a momentum larger than .75 P_i is selected as follows : the quantity "D", defined page 6, is given by the formula $D = \alpha A - B$ with α, A and B defined on Fig. 4a. The correlation between D and $P_{forward}$ is given on Fig. 4b for inelastic events $\pi p \longrightarrow pX$. The elastic events have $D_{min} \leqslant D \leqslant D_{max}$ and more precisely in the plane (A, B) these events are located in a narrow band Fig. 4c. A majority encoder logic (MECL 10000 series) operating on H3, PC1, PC2 gives the pattern of the forward proton trajectory expressed by the 2 quantities A and B, this is used as an address to get a one or a zero from a programable memory 25 Kbits large which is the image of the plane A, B. This needs only 200 chips also in the 10000 MECL series because the elastic zone where the bit is set at one is very narrow (5 mm). The full time for the processing is 50 ns per event.

The counter C4 has a hole in order to let the beam through. In the case of negatively charged incident particles this hole lies outside the impact of the scattered protons. With a positive beam the loss of efficiency near u_{min} is small (Fig. 5). This is due to the large spread in C4 of the scattered proton with respect to

the hole size. The chamber PC2 has a dead zone in front of the hole. PC1 has a dead zone in the path of the beam. If H_3 is a proportional chamber, it will also have a dead zone. We have included in the geometrical efficiency curves of figure 5 the effect of these dead zones.

Triggers will be caused by inelastic channels having a fast, forward proton. We estimate the trigger rate at 60 GeV/c caused by these channels by assuming that the shape of the mass spectrum of the backward meson system recoiling from the proton has an s dependence given by the data at 8 and16 GeV/c [7]. Taking the momentum acceptance of our forward spectrometer to be $\geq \frac{3p}{4}$ and making a reasonable estimate for the s-dependence of the backward elastic peak [8] we find a trigger rate of I80 triggers/puls 40 GeV/c. We interpret this trigger rate as an upper limit, as the requirements of a backward pion and an absence of counts in the anti-counters have not been imposed. With these requirements we believe the trigger rate should be divided by a factor 5, at least.

δ rays energetic enough to reach the second proportional chamber in Goliath occur for 8 % of the beam. Depending on the amount of hydrogen traversed , these δ rays will cause some triggers. δ rays which accompany elastic events will be filtered in the analysis.

Our data handling system will be designed to handle 450 events per spill, a number more than an order of magnitude higher than the trigger rate which we expect to have. In order to give an idea of the amount of data which must be handled in this experiment, we use the following figures :

- number of wires : 22900 ;
- number of hodoscope elements : 414 ;
- number of wire pulses/event : 70 ;
- maximum number of events per spill : 450.

The information in the chambers is transfered in sequence onto a bus line by means of 8-bit words at each pulse of a ten megacycle clock. The total transfer time is ten microseconds. These data will be encoded into 70 16-bit words. An additional 16 words are used for

Special fast electronics connected to the two wire planes of the second chamber as well as a simple treatment by the computer will allow rough checks for good spatial and kinematical correlations. This will permit us to do a pattern filter for the events before storage on magnetic tape for later off-line analysis.

The yield of elastic scattering events can be estimated by fitting low energy data and extrapolating the fit to high energy using a parametrization consistent with Regge behaviour. [8]. The efficiency of our system varies smoothly with u. The overall azimuthal acceptance is typically 33 % at 40 GeV/c and increases with s. Assuming an 8 % loss due to final state interactions, we have a global efficiency which varies from 21 to 34 %. Using the estimated H_1 beam characteristics, [9] the yield of backward elastic events can be determined. These yield results, based on a 100 hr running period and a security factor of .5, are given in the following table. (We take a maximum of 10^7 particles/pulse. The table indicates the number of primary protons which are needed at each momentum, as well as other relevant data mentioned above).

Momentum (GeV/c)	Global apparatus efficiency	π or K^s /burst	primary protons per burst	σ_{pb}	Yield/100 hours
25	.25	8.4×10^6	10^{11}	45.	2.8×10^4
π^+ 40	.34	6.6×10^6	5×10^{10}	9.5	6.3×10^3
75	.37	4.0×10^6	10^{10}	1.8	7.2×10^2
120	.37	1.0×10^6	10^{10}	0.6	6.6×10^1
25	.23	9.6×10^6	10^{11}	45.	$3. \times 10^4$
π^- 40	.32	9.6×10^6	10^{11}	14.	1.3×10^4
75	.35	9.7×10^6	10^{11}	4.	4.1×10^3
120	.35	9.9×10^6	5.10^{11}	1.6	1.7×10^3
25	.24	4.6×10^5	same	15.	500.
K^+ 40	.31	3.7×10^5	as	2.6	90.
75	.33	2.1×10^5	π^+	0.3	10.

Thus with 800 hours of running, or 100 8-hour shifts, we will obtain 1000 to 30 000 backward elastic events at each of three momenta for π^+p and π^-p and up to 500 for K^+p. We see clearly that the primary proton number required is low enough to allow an efficient work with a new-born machine.

With our trigger condition and off line pattern filter (hardware and software on PDP II-45), we can estimate that the number of events to be handled with a CDC 7600 computer would be about $2*10^6$. The determination of momenta and angles of the tracks in an inhomogeneous magnetic field and the fit takes .1 s per event and the pattern .05 s as indicated by pattern simulation, this will [illegible] between 80 to 100 hours of CDC 7600.*

In order to estimate the background in our final data sample, we have written an analysis program for the experiment and have used it to fit elastic and inelastic events generated by a Monte Carlo program. (This program was used to determine the spatial and angular resolution of the forward and backward arms.). The reaction most likely to simulate elastic scattering is the production of a backward meson system with low effective mass. We find that for a meson effective mass in the range .285 to .55 GeV, the probability of being a background event (i.e., surviving the χ^2 cuts determined by fitting elastic events) is 2 %. (Fig. 6). For higher masses (1.0 to 1.2 GeV), this probability drops to .5 %. Based on the 16 GeV/c data [7] and on the faith that nature is not cruel, we expect to encounter background at the few percent level ; of course, if the background is an order of magnitude worse than this, we could subtract it accurately enough so that the resulting systematic error would be small compared to the statistical error.

* i.e. 10% of this time on the CERN's 7600 and 90% on the Saclay's 7600.

ADDITIONAL PHYSICS OBJECTIVES

During the experiment on backward πp scattering we will simultaneously collect data on very interesting backward reactions. The reactions we would like to study are :

$$\bar{p}p \rightarrow \pi^{\pm}\pi^{\mp}$$

$$\bar{p}p \rightarrow K^{-}K^{+}$$

They need a parallel trigger system where Cerenkov counters are in coincidence.

Reactions involving baryon decay with a π° and a fast forward proton could be reached with our apparatus:

$$\pi^{\pm}p \rightarrow N^{*}\pi^{\pm}$$
$$\hookrightarrow p\pi^{\circ}$$

$$\pi^{+}p \rightarrow \Sigma^{+}K^{+}$$
$$\hookrightarrow p\pi^{\circ}$$

$$K^{-}p \rightarrow \Sigma^{+}\pi^{-}$$
$$\hookrightarrow p\pi^{\circ}$$

We have run our Monte-Carlo programm with the reaction $\pi^{+}p \rightarrow N^{*+}\pi^{+}$, $\hookrightarrow p\pi^{\circ}$ the N* having no width.
Then, we have performed on these events a fit for the reaction $\pi^{+}P \rightarrow p\pi^{\circ}\pi^{+}$ without the knowledge of the p, λ, φ, of the π°, we have found an effective mass for the system $p\pi^{\circ}$ having the mass of the N* for mean value, and a full width of 35 Mev. Then we anticipate that we are able by 1C fit to study inelastic reactions with one missing π°.

The reactions $\pi^{\pm}p \rightarrow p, \rho^{\pm}, A_1^{\pm}, A_2^{\pm}, B^{\pm}$ are also attainable in the same may.

The use of a target filled with Deuterium allows us to measure reactions as :

$$K^{+}n \rightarrow pK^{\circ}$$
$$\hookrightarrow \pi^{+}\pi^{-}$$

$$\pi^{+}n \rightarrow p\rho^{\circ}$$
$$\hookrightarrow \pi^{+}\pi^{-}$$

$$\pi^{+}n \rightarrow p\pi^{\circ}$$

$$\pi^{+}n \rightarrow p\eta^{\circ}$$

For the two last reactions producing a π° or a η° five lead plates

After the elastic cross-section measurements we intend to replace the hydrogen target by a polarized target without changing anything else in the apparatus. In this case the measurable domain shrinks ($|u|_{max} \simeq 0.7$ instead of 1.1). However, essential information will be gained with regard to the confused situation in the baryon exchange of natural and unnatural parity.

A careful examination of the possibility of using a polarized target in our magnet has shown that the best way is to use a conventional butanol polarized target. This implies the use of shims of limited size in order to have a $dB/B = 4.10^{-4}$. The homogeneity of the field in the momentum measurement region is not drastically altered. Goliath would be powered with 2.5 MW. With the 18 kG field the butanol target will reach a 70 % polarization. The shimed magnet and the polari target are sketched in fig. 7. With a target of 20 cm long the interaction rate is 3.5 times less than with our hydrogen target.

If the kinematical constraints given by the apparatus do not allow a clean rejection of events produced on bound protons from those produced on free polarized protons, the polarization measurement is still possible by the substraction method. In that case the accuracy on P is given roughly by

$$\Delta P \simeq \frac{1}{P_t} \sqrt{\frac{2}{\rho \cdot N_H}}$$

where ρ is the ratio of events on free protons to events on free + bound nucleons fitting elastic scattering, P_t is the target polarization and N_H the number of events on free protons. Monte Carlo calculations using the above mentionned resolutions show that $\rho \simeq 0.7$ instead of $\rho = .25$ when the events on free protons cannot be separated by fit.

For the reactions, more complex, in which the final state meson does not have zero spin, the separation of the exchange naturality states can be performed by the study of its spin states using the density matrix elements measured in an appropriate frame (transversity frame). The reactions as $\pi^+ p \to \Sigma^+ K^+$ or $K^- p \to \Sigma^+ \pi^-$ where the

LOGISTICS

We would like CERN to provide :
- Cerenkov counters for the beam particle identification ;
- the power supplies for the Goliath and Mimosa magnets

The Goliath magnet floor surface is 4.8 x 4.8 m^2 ; the gap center is 154 cm above the ground ; this takes into account the tripod which is 23 cm high and can be removed if necessary. At full power the running voltage is 600 V and the water cooling system requires 80 m^3 at 22 kg/cm^2. The total weight is 250 metric tons.

The Mimosa magnet which could be loaned from the Saturne Department has the overall dimensions of 303 cm x 155 cm x 245 cm. For a field of 1.4 T, the voltage is 290 V with a power of 150 KW. The water pressure is 15 kg/cm^2 at 3.5 m^3/h delivery.

We will provide :
- all the phototubes and scintillators ;
- the proportionnal chambers ;
- the downstream Cerenkov counters ;
- associated electronics and cables ;
- the targets ;
- the computer (PDP 11-45).

All the electronic equipment including the PDP 11-45 computer, the tape units, the teletype and the other displays would be installed in a trailer. The total floor area required is approximately 9 x 25 m^2.

The construction of the different parts of the apparatus could be achieved by the begining of 1975. We intend to do a complete test of the whole apparatus by measuring backward scattering at lower energies. Then we will be ready to run in the SPS West Hall by mid 76 with an [illegible] fully tested.

REFERENCES

1. R. P. Feynman, Phys. Rev. Letters 23, 1415 (1969).

2. R. P. Feynman, private communication.

3. E. L. Berger and G. C. Fox, Nuclear Physics B26, 1 (1971).

4. J. P. Chandler, R. R. Crittenden, K. F. Galloway, R. M. Heinz, H. A. Neal, K. A. Potocki, W. F. Prickett, and R. A. Sidwell, Phys. Rev. Letters 23, 186 (1969).

5. S-Y Chu and A. Hendry, Phys. Rev. Letters 25, 313 (1970) and Phys. Rev. D4, 2743 (1971).

6. S-Y Chu and A. Hendry, to be published.

7. E. W. Anderson et al., Phys. Rev. Letters 22, 1390 (1969) and Phys. Rev. Letters 22, 102 (1969).

8. F. Hayot, private communication.

9. SPS Experimental facilities CERN/SPSC/T 73-9.

FIGURE CAPTIONS

FIGURE 1 Side and top views of the apparatus

- H_0, H_1, H_2, H_3 : scintillator counter hodoscopes

- PC 1, PC 2 : proportional wire chambers

- TC 1, TC 2 : atmospheric pressure gas Cerenkov counters

- AC I, AC 2, AC 3 : anticoincidence counters

- C4 : forward scattered proton coincidence counter.

The beam dispersion corresponds to the gray zone. The forward scattered proton for p = 80 GeV/c and for $0 > u > -1.3$ $(GeV/c)^2$ covers the hatched zone.

FIGURE 2 Goliath with shims and a polarized target.

FIGURE 3 Magnetization curve of the Goliath magnet.

FIGURE 4 a) Meaning of α, A, B (see text page 8)

b) "D" versus $P_{forward}$

FIGURE 5 Global detection efficiencies of the apparatus as computed by Monte-Carlo. Solid and dashed lines refer to $\pi^- p \rightarrow p\ \pi^-$ and $\pi^+ p \rightarrow p\ \pi^+$ respectively.

FIGURE 6 Distribution of the χ^2 for the fit of $\pi^- p \rightarrow p\ \pi^-$

a) for elastic events $\pi^- p \rightarrow p\ \pi^-$

b) for inelastic events $\pi^- p \rightarrow p\ \pi^- \pi^o$ $(0.300 < M_{\pi^- \pi^o} < 0.700)$ with π^o not seen and not included in the fit.

FIGURE 7 Goliath magnet with shims and a polarized target.

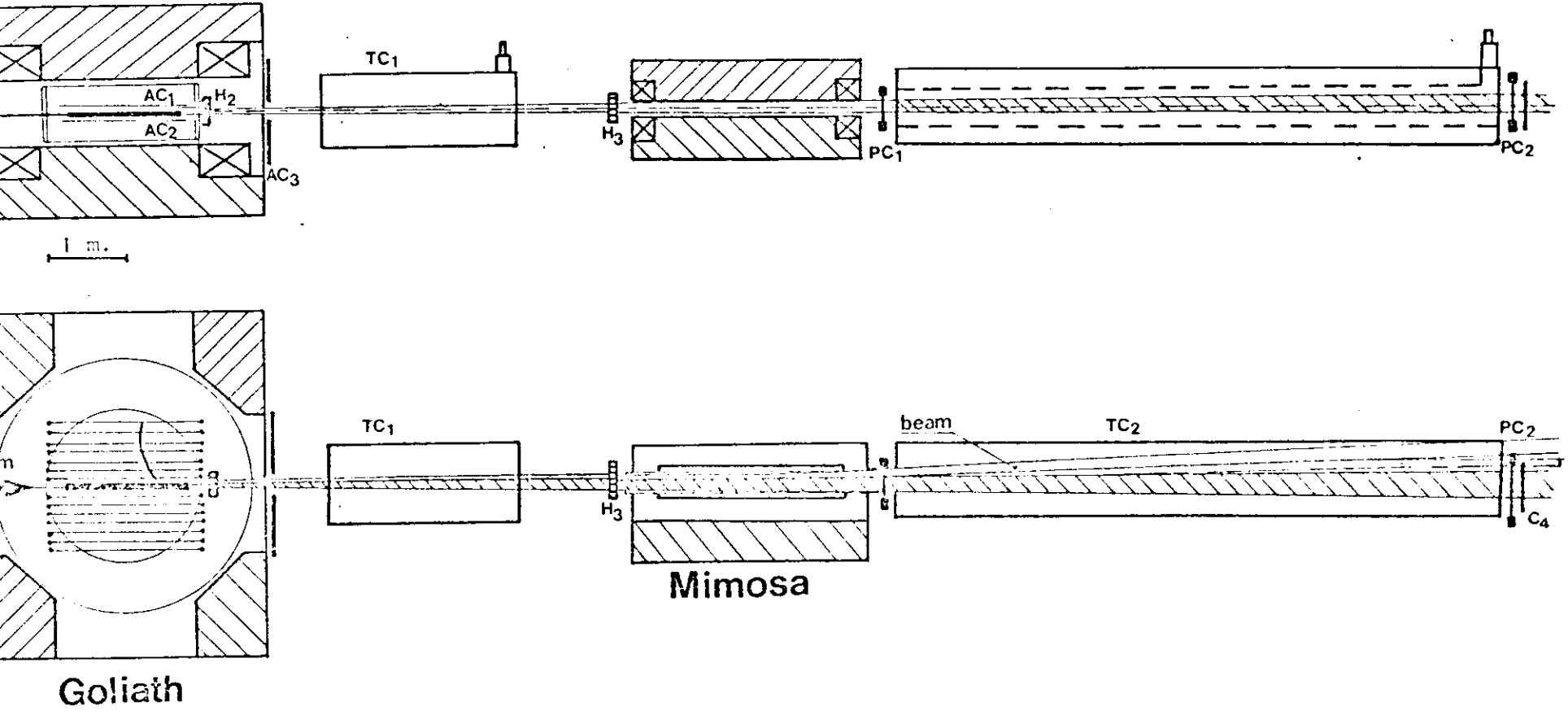
AC1
H2
AC2
AC3
TC1
H3
PC1
PC2
1 m.
TC1
beam
TC2
PC2
H3
C4
Mimosa
Goliath

Fig 1

t. view | ½ section c

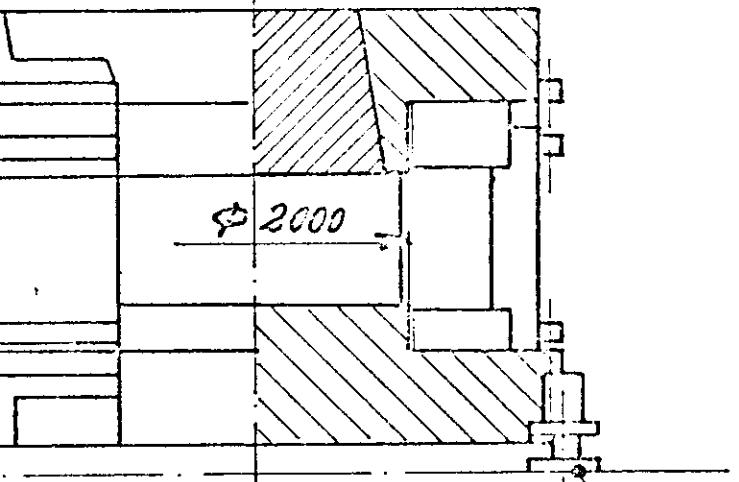

raulic jacks allowing
ove the magnet a few
ers a day.

LIATH" MAGNET.

gap height is now extended
metre.

be taken into pieces
20 metric tons.

½ section b | ½ ext. view

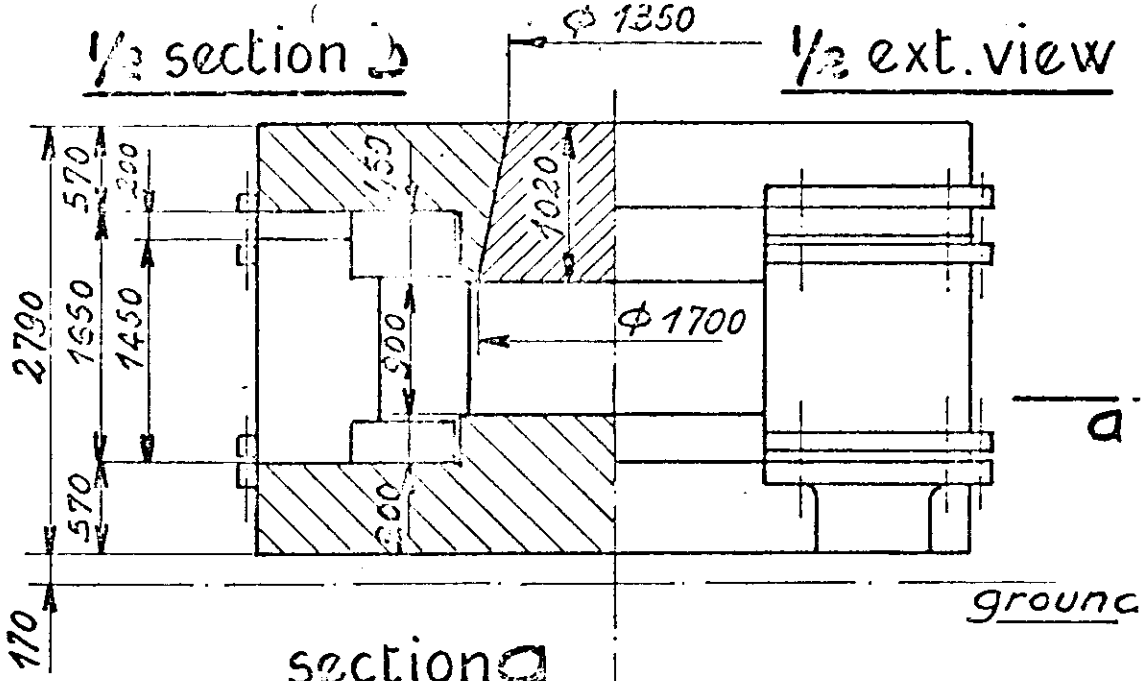

section a

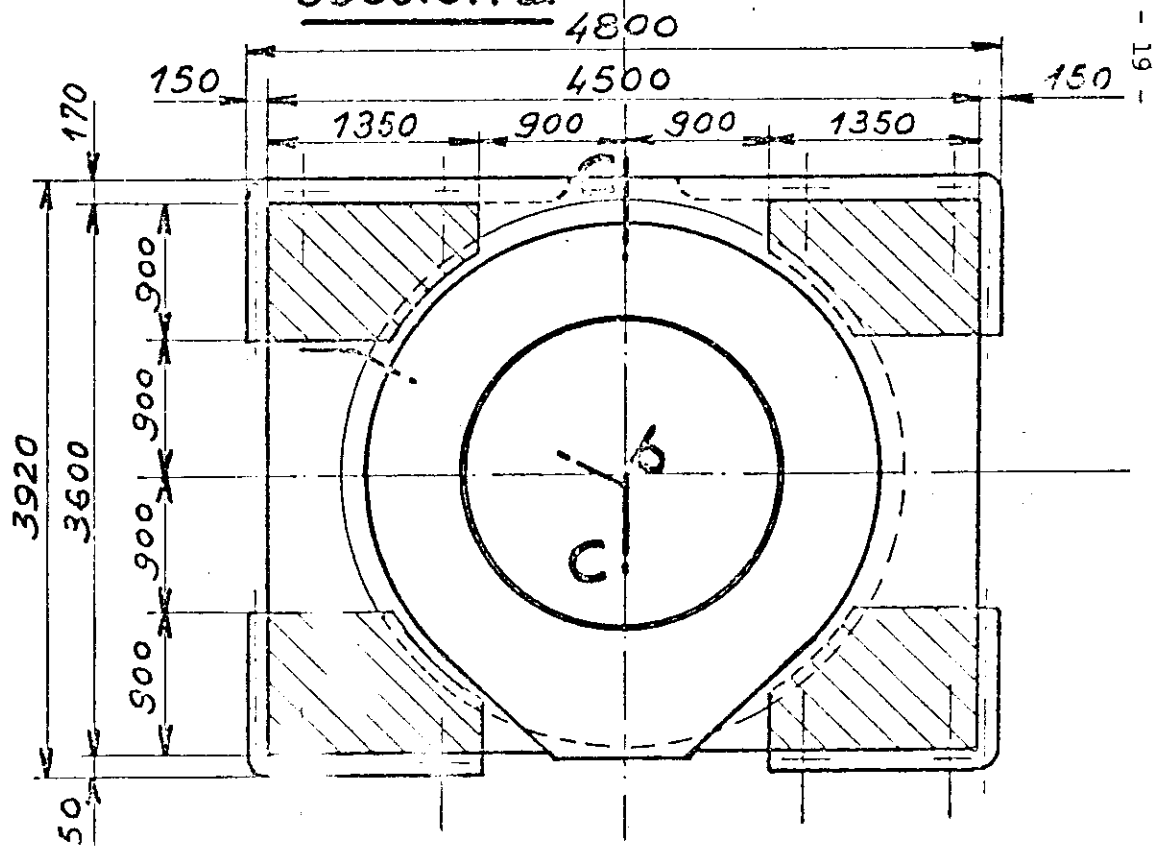

fig.2

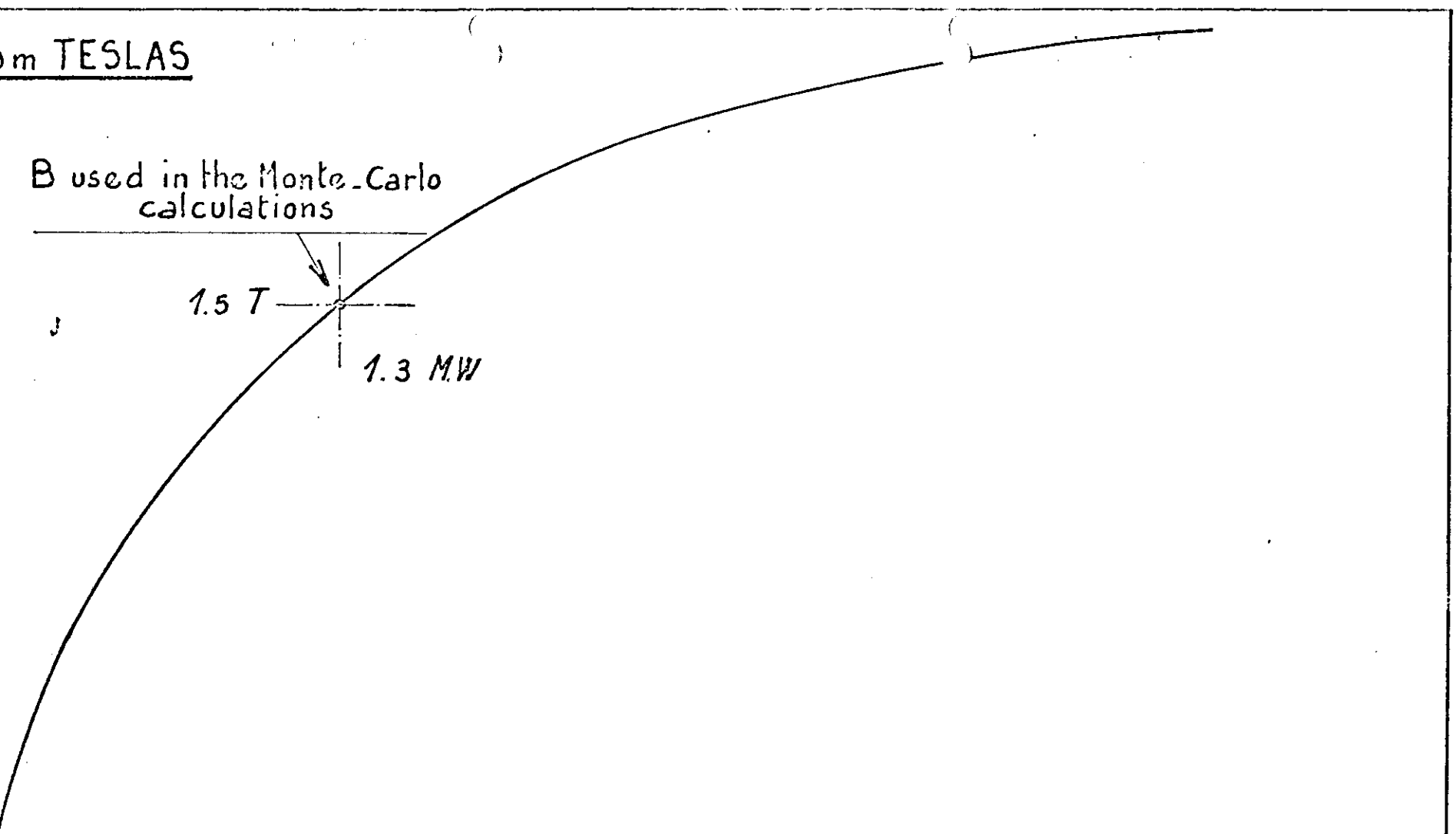

"Goliath" MAGNETIZATION CURVE FOR 1,05m GAP HEIGHT

fig.3

P. M. WATTS

D-P CORRELATION FOR INELASTIC EVENTS.

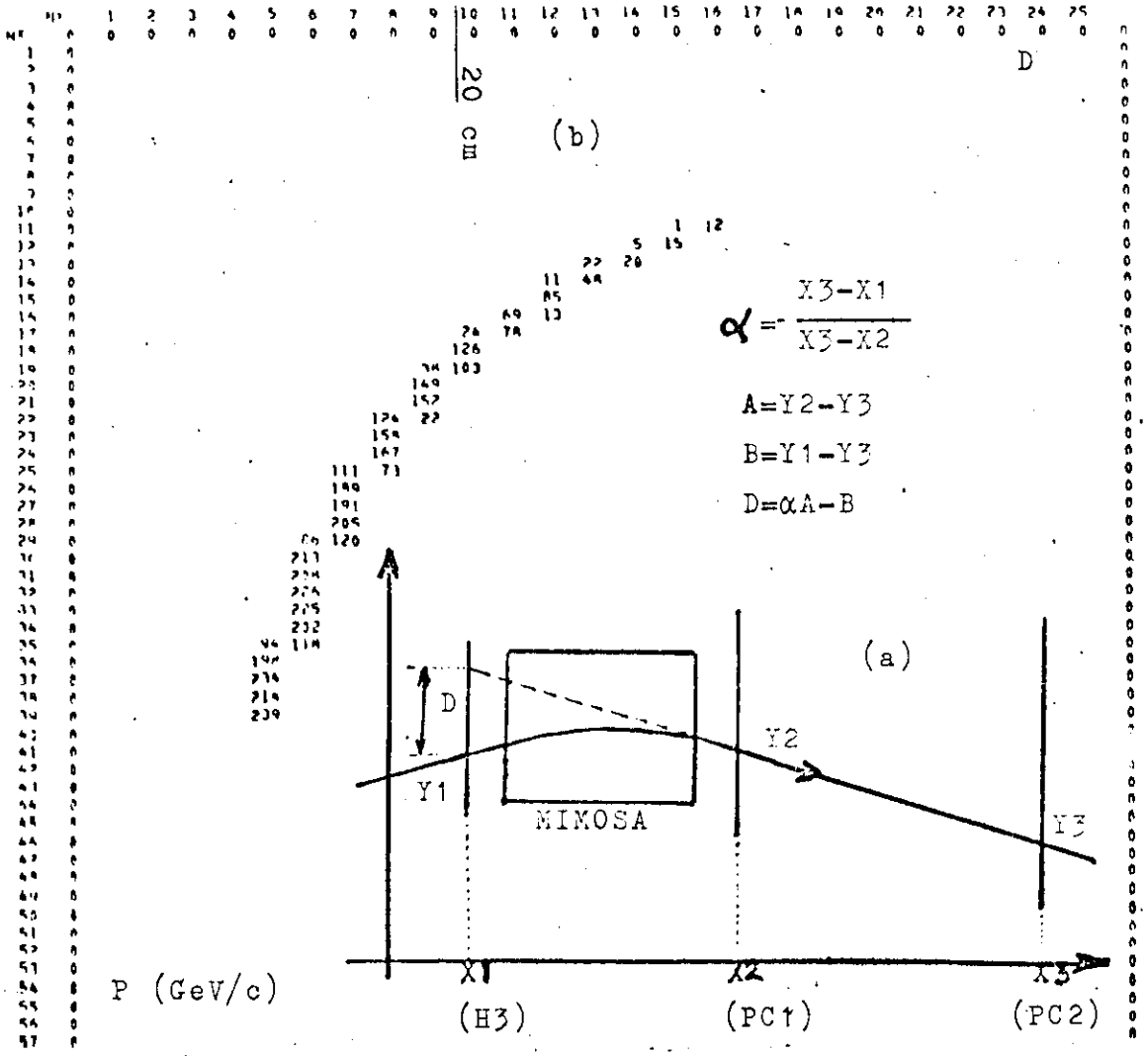

DIAGRAMME 2 AMAS 371/AMAS 301

CORRELATION 036 024

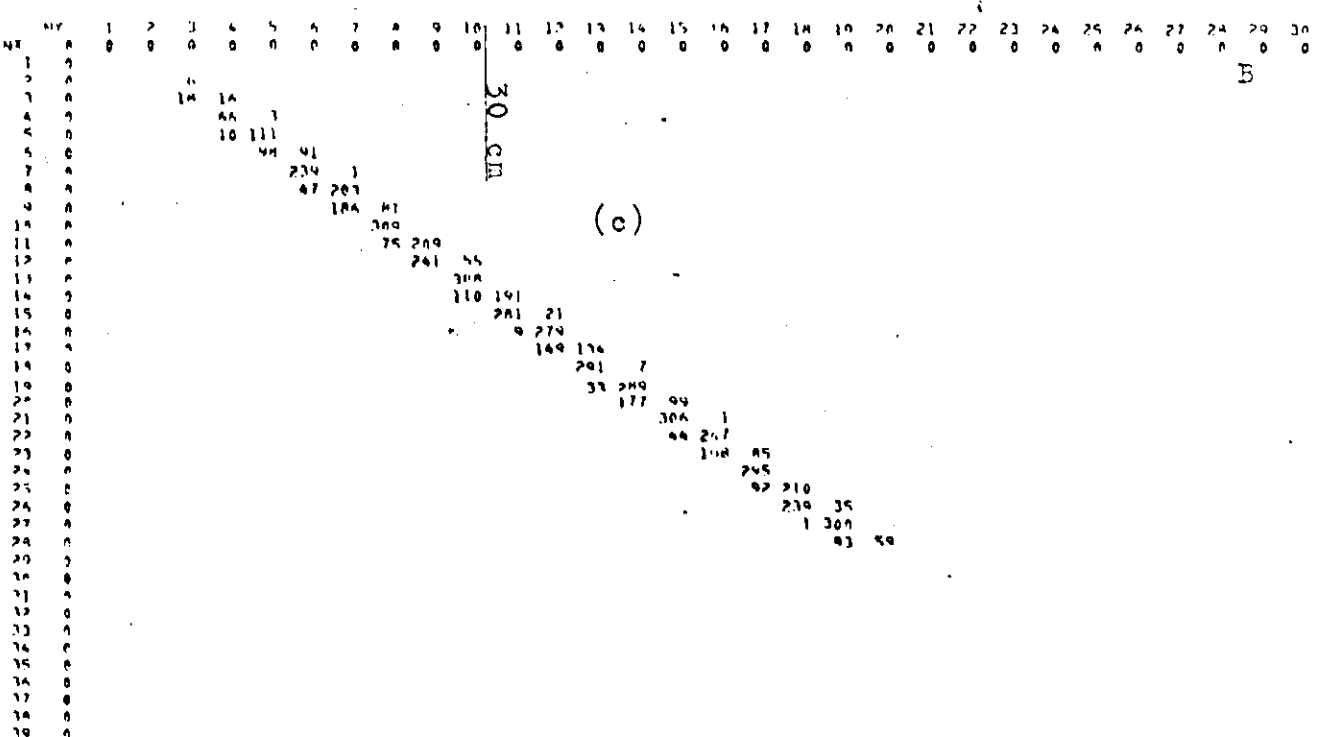

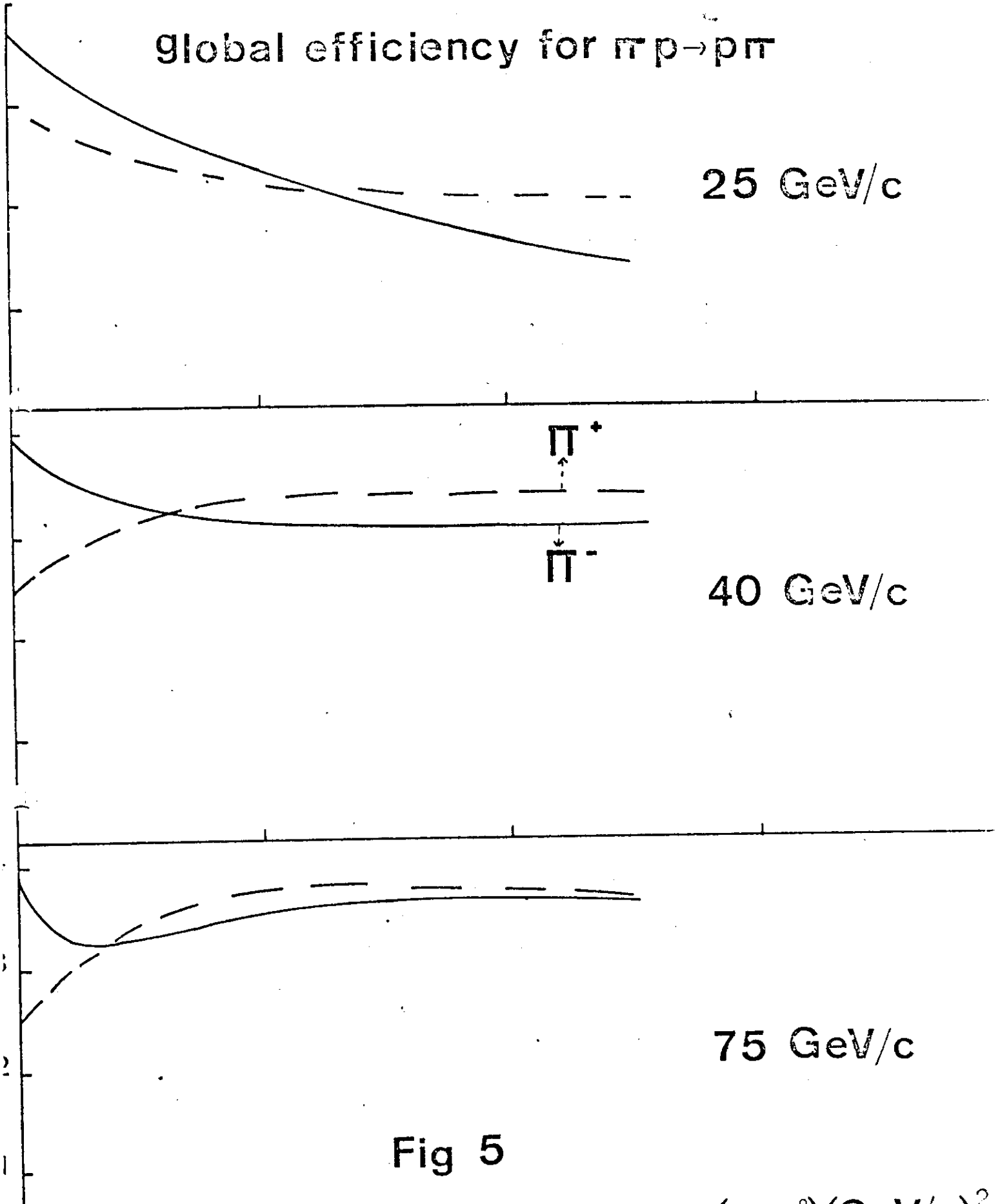

Fig 5

```
MASTER TESTS   11 -
XLOC  412

 BITS BINS  CAP.  LOST    NX    DELX    XLOW       XMEAN     XRMS  CONTENT  EXCL.  U-FLOW  O-FLOW
  10     6  1023     0    25     4.      0.       2.8134    2.745    721.               0.      0.    721 ENTRIES IN ALL.

                                                                                          MULTIPLY PLOT BY   10** 1

  58  4                  8
  56  X                  6
  54  X                  4
  52  X                  2
  50  X                  0
  48  X                  8
  46  X                  6
  44  X                  4
  42  X                  2
  40  X                  0
  38  X                  8
  36  X                  6
  34  X                  4
  32  X                  2
  30  X                  0
  28  X                  8
  26  X                  6
  24  X                  4
  22  X                  2
  20  X                  0
  18  X                  8
  16  X                  6
  14  X1                 4
  12  XX                 2
  10  XX                 0
   8  XX                 8
   6  XX                 6
   4  XX1                4
   2  XXX2 000           2

CON-    51
TENT    622

        923401110

BIN
NOS     123456789

LOW       112223
BIN     482604826
EDGE  .

BLS HGR  51           I+51       ICHI2   FOR INELASTIC EVENTS
                      ----------------------------------------------------------------------------------------------

MASTER TESTS   12 -
XLOC  412

 BITS BINS  CAP.  LOST    NX    DELX    XLOW       XMEAN     XRMS  CONTENT  EXCL.  U-FLOW  O-FLOW
  10     6  1023     0   100     4.      0.      106.52   90.259    335.               0.    355.    690 ENTRIES IN ALL.


                                                                                                            8
  18        X                                                                                               7
  17        X                                                                                               6
  16        X                                                                                               5
  15     X  X X                                                                                             4
  14     X  X X                                                                                             3
  13     X  X X                                                                                             2
  12     X  X X X                                                                                           1
  11     X  X X X                                                                                           0
  10     X  X X X    X   X                                                                                  9
   9     X XX XXX    X   X                                                                                  8
   8  X XXXXX XXX    X   X X                                                                                7
   7  XXXXXXX XXX   XX X X X                                                                                6
   6  XXXXXXX XXX  XXXXX X X X      X                     X                                                 5
   5  XXXXXXXXXXXXXXXXXX X X XXX   XX X  X      X     X    X                                                4
   4  XXXXXXXXXXXXXXXXXX X XXXXX  XXX X  XXX   X X    X    X   X                X                           3
   3  XXXXXXXXXXXXXXXXXXXXXXXXXX  XXXXX  XXX X X X X XX X X    X XX   X         X        X                   2
   2  XXXXXXXXXXXXXXXXXXXXXXXXXXX XXXXXXX XXXXX X XXXXXXXXXX XXXX XX X X XXX    X        X                   1
   1  XXXXXXXXXXXXXXXXXXXXXXXXXXX XXXXXXXXXXXXX X XXXXXXXXXX XXXXXXX XXXXXXX X  XX XX   X X  X   X X XX

CON-     1  1 1 1    1  1
TENT  875883355125556706730344655 2465352154423 5 4232352323 2223136 21412221 1  31 11  4 1   1  1 1 11

BIN            1         2         3         4         5         6         7         8         9
NOS   1234567890123456789012345678901234567890123456789012345678901234567890123456789012345678901234567

                                 1111111111111111111111111112222222222222222222222222223333333333333333333333
LOW
BIN         11222334445556667788899000111222334445556677888990001122233444555666778889900011222334445566677 88
EDGE  482604826048260482604826048260482604826048260482604826048260482604826048260482604826048260482604
```

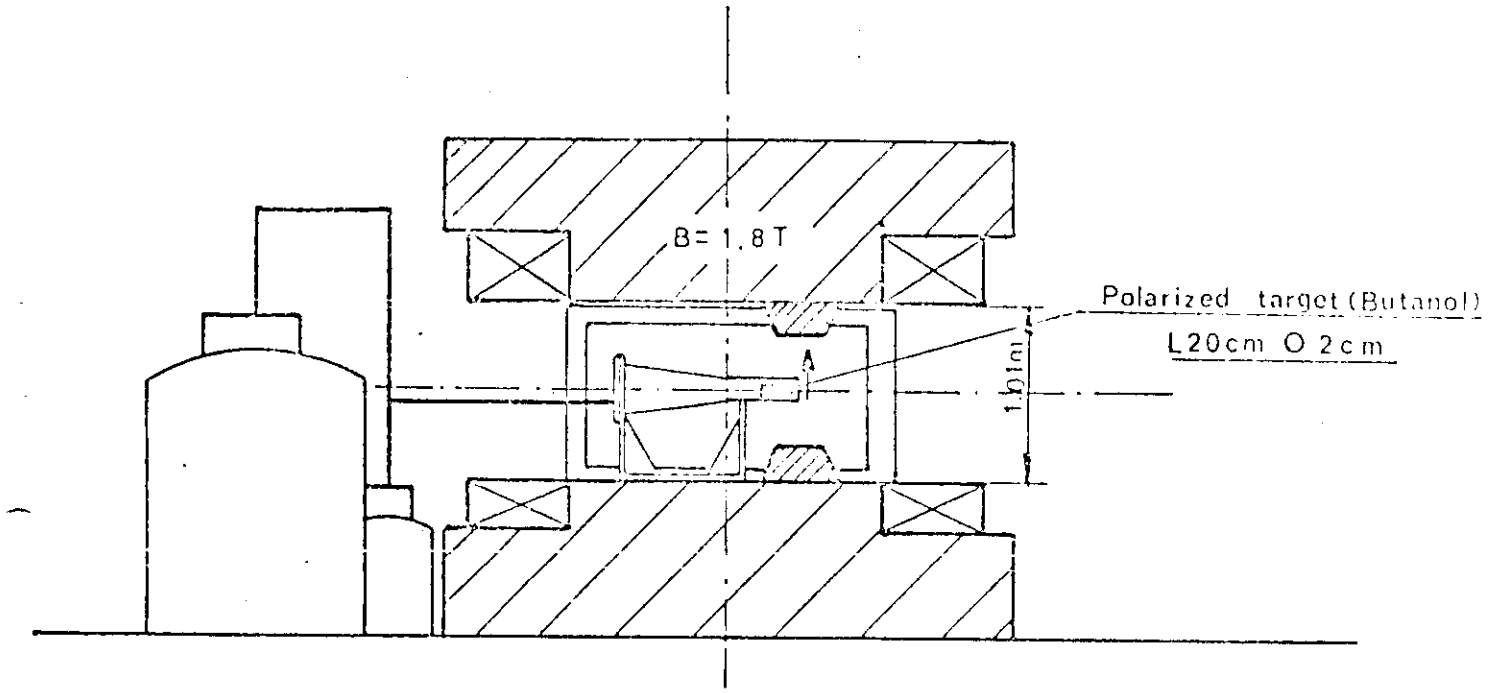
B= 1.8 T
Polarized target (Butanol)
L 20cm O 2cm
1.0 1m

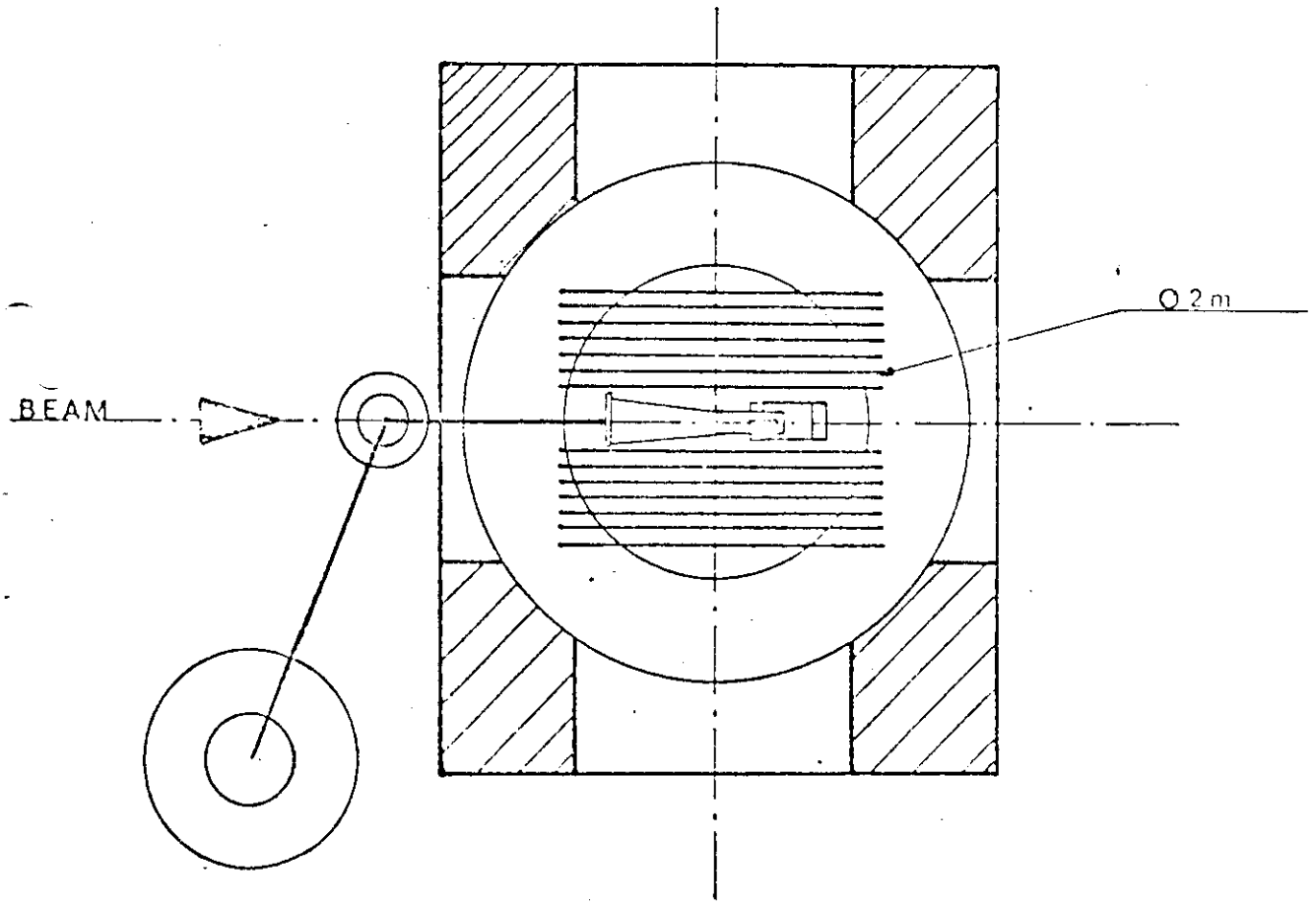
O 2m
BEAM

APPENDIX I

CERENKOV COUNTERS

We need threshold Cerenkov counters in order to separate protons from π, K mesons with a global inefficiency of about 10^{-6} - 10^{-7} for momenta ranging from 20 to 100 GeV/c.

This inefficiency implies that a minimum number of photo electrons are recorded by the phototube :

$$\varepsilon_{in} = e^{-N}$$

$$\varepsilon_{in} = 10^{-6} \qquad N = 13.5$$

$$\varepsilon_{in} = 10^{-7} \qquad N = 16$$

N results from Cerenkov light emitted by particules of mass m, with a momentum p in a gas radiator of refraction index n and length L.

For large momenta the number of photoelectron is :

$$N = K\ L\ \theta^2$$

$$\text{with } \theta^2 = 2\ (n-1) - \frac{m^2}{p^2}$$

The value of K is 150 which corresponds to the detection of Cerenkov radiation between 2200 Å and 5500 Å, to a 15% conversion ratio of Cerenkov photons into photoelectrons and to a 80% reflectivity ratio of the mirror.

$$K\ \text{ph/cm} = \frac{2\pi}{137}\left[\frac{1}{2200} - \frac{1}{5500}\right] 10^8 \times \frac{15}{100} \times \frac{80}{100} = 150$$

The length is computed using $L = \frac{N}{K\ \theta^2}$

For instance at 100 GeV/c one gets

$\varepsilon_{in} = 10^{-6}$ with L = 14.5 meters

$\varepsilon_{in} = 10^{-7}$ with L = 17 meters

The radiation length choosen is 12 m , made of two modules :

TC I = 4 m (in Mimosa magnet) (Fig. 3)

TC 2 = 8 m (Fig. 4)

We will use gases at atmosphere pressure :

Gas	$(n-1) \times 10^6$	P range GeV/c	C used	Inefficiency π, K , /p separation
CO_2	450	20 - 30	TC_I	10^{-7}
N_2	297	27 - 39	TC_I	10^{-7}
H	135	37 - 56	$TC_I + TC_2$	10^{-7}
Ne	67	66 - 81	$TC_I + TC_2$	10^{-6}
		75 - 81		10^{-7}
He	35	≃ 110	$TC_I + TC_2^*$	$\simeq 10^{-5}$

We may avoid the use of hydrogen above 40 GeV/c by using a mixture of He - N_2 or Ne - N_2 so we can achieve an inefficiency of

10^{-6} up to 95 GeV/c

10^{-7} up to 81 GeV/c

We will need a refractometer in order to measure the refraction index with a precision of $5 \cdot 10^{-6}$.

Optical design

The shape of the mirrors is essentially determined by detailed and realistic Monte-Carlo study. We simulate first the elastic and inelastic scattering and retain the particles which go through the trigger defined by H_2, H_3, PC_1, PC_2. Then we make a random photon emission at the proper Cerenkov angle along their trajectories. For the first Cerenkov we have taken into account the Mimosa magnetic field. The trajectories of the photons are followed through the optical system and therely we determine the final number which are detected by the photomultiplier tube (RTC XP 2020, RCA 31000...).

The optimization shows that the best shape of the mirrors is a part of an ellipsoid. They will be machined from acrylic plastic. Since the photon spectrum from Cerenkov radiation is proportional to $1/\lambda^2$ they will be coated with a thin U - V aluminium deposit. We hope to have a reflectivity of the mirrors bigger than 80% for wavelength down to 2200 Å. For the same reason, phototubes will have quartz windows. All gases have a good transmission for ultraviolet frequencies. The possible prompt scintillation which is isotropic seems not to be important but an estimation may be done be placing the Cerenkov counter with particle entering through the exit window.

On figure 1 one reports for three energies the impact of the triggered particles on the entrance windowof TC_1 and TC_2, the Monte-Carlo impact of the photons on the elliptic mirrors and the light-spot on the photomultiplier window. On figure 2 is plotted the computed inefficiency versus the momentum at two incident energies.

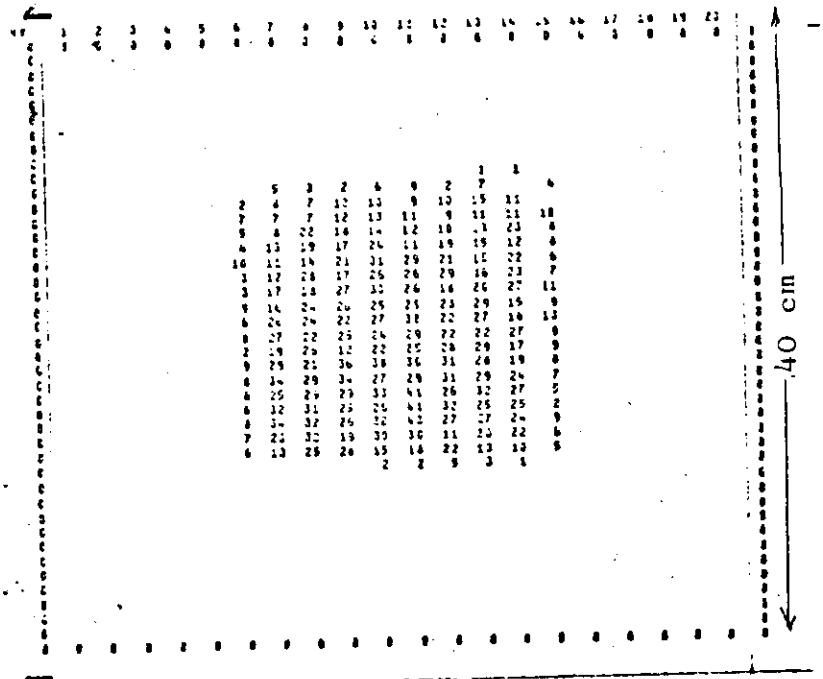

25 GeV/c

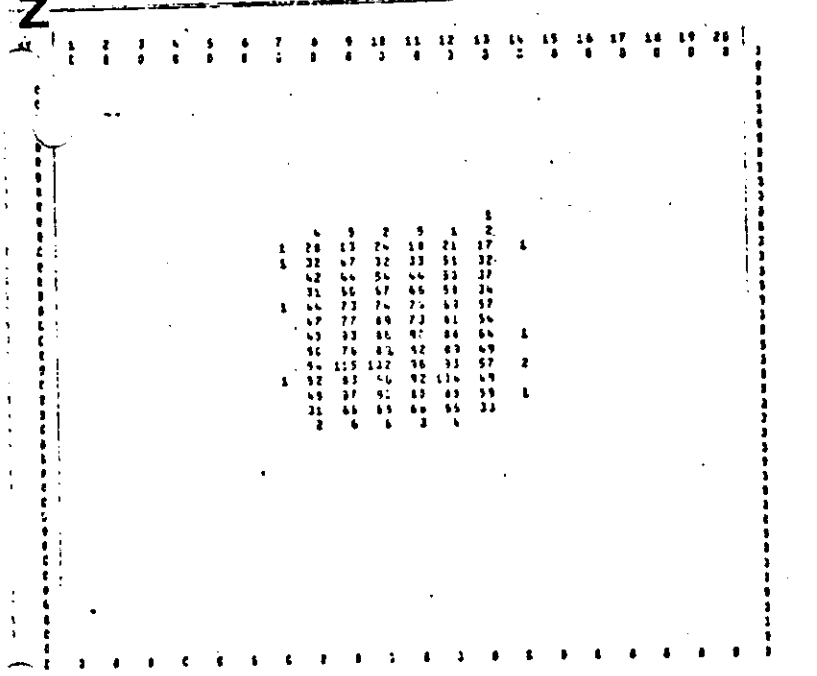

40 GeV/c

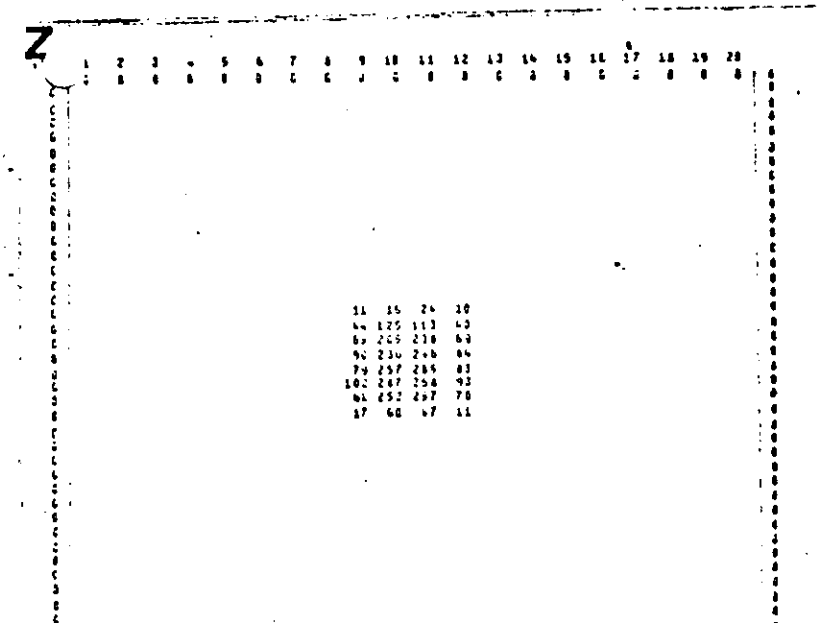

75 GeV/c

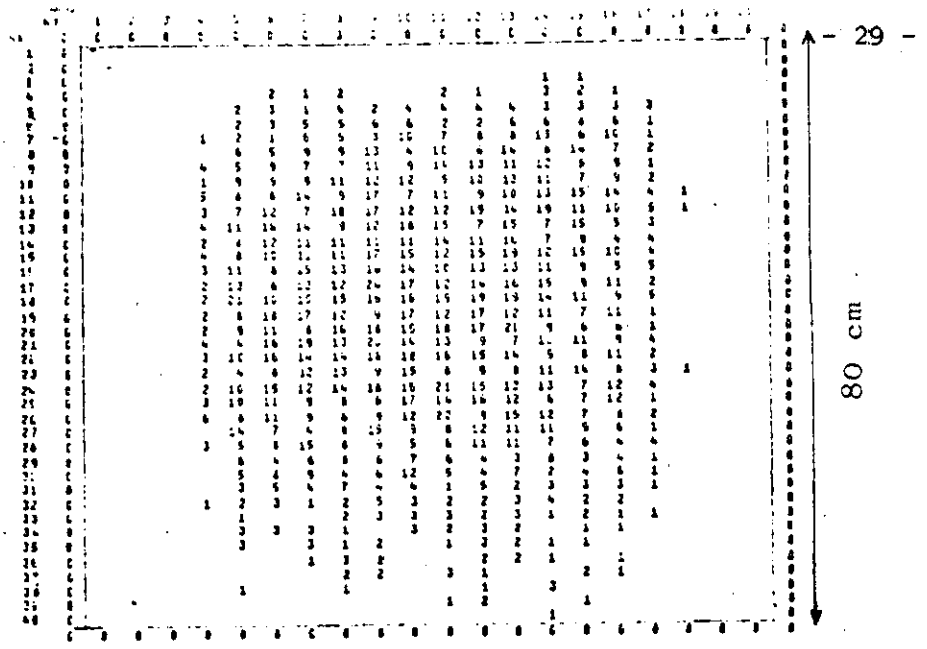

25 Gev/c

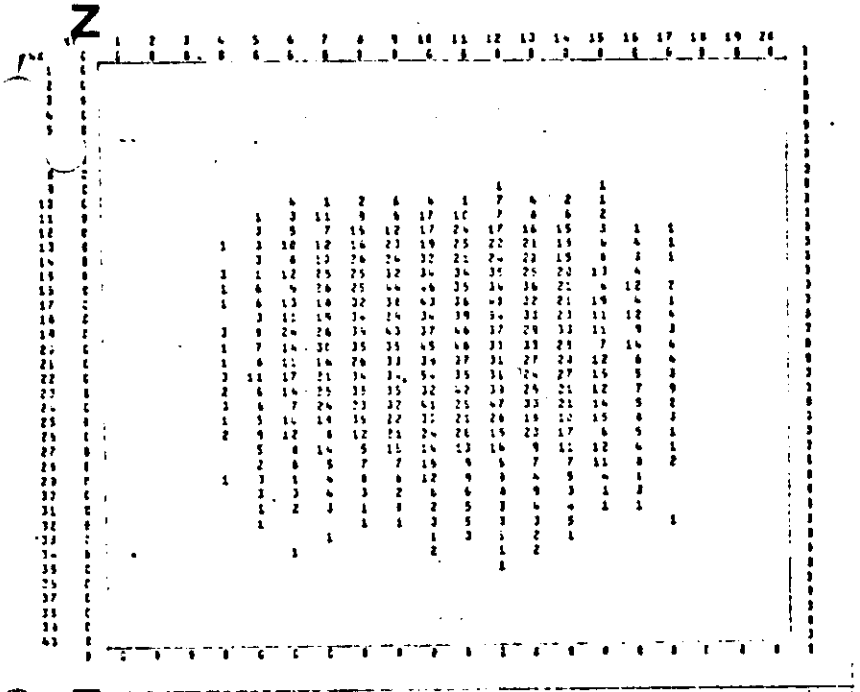

40 Gev/c

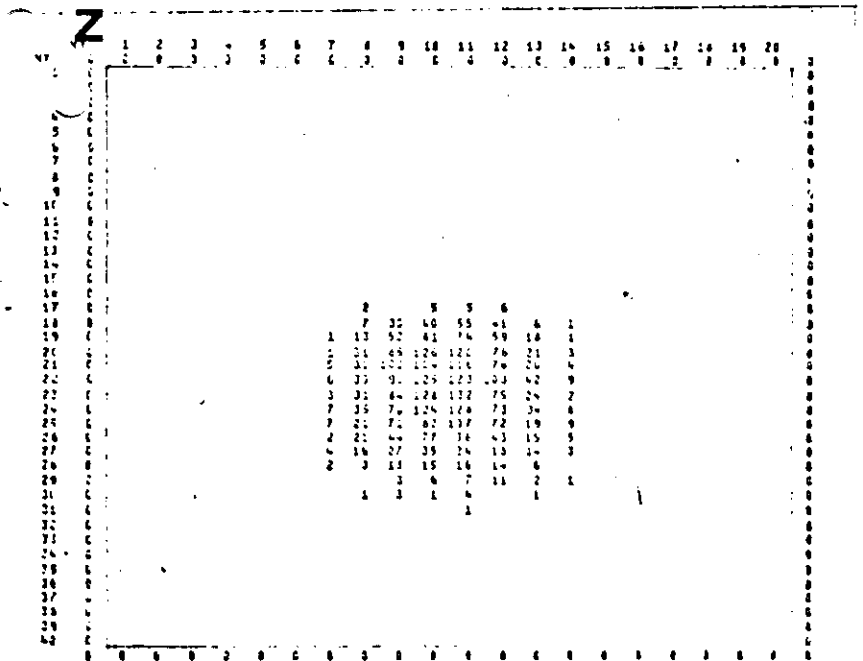

75 Gev/c

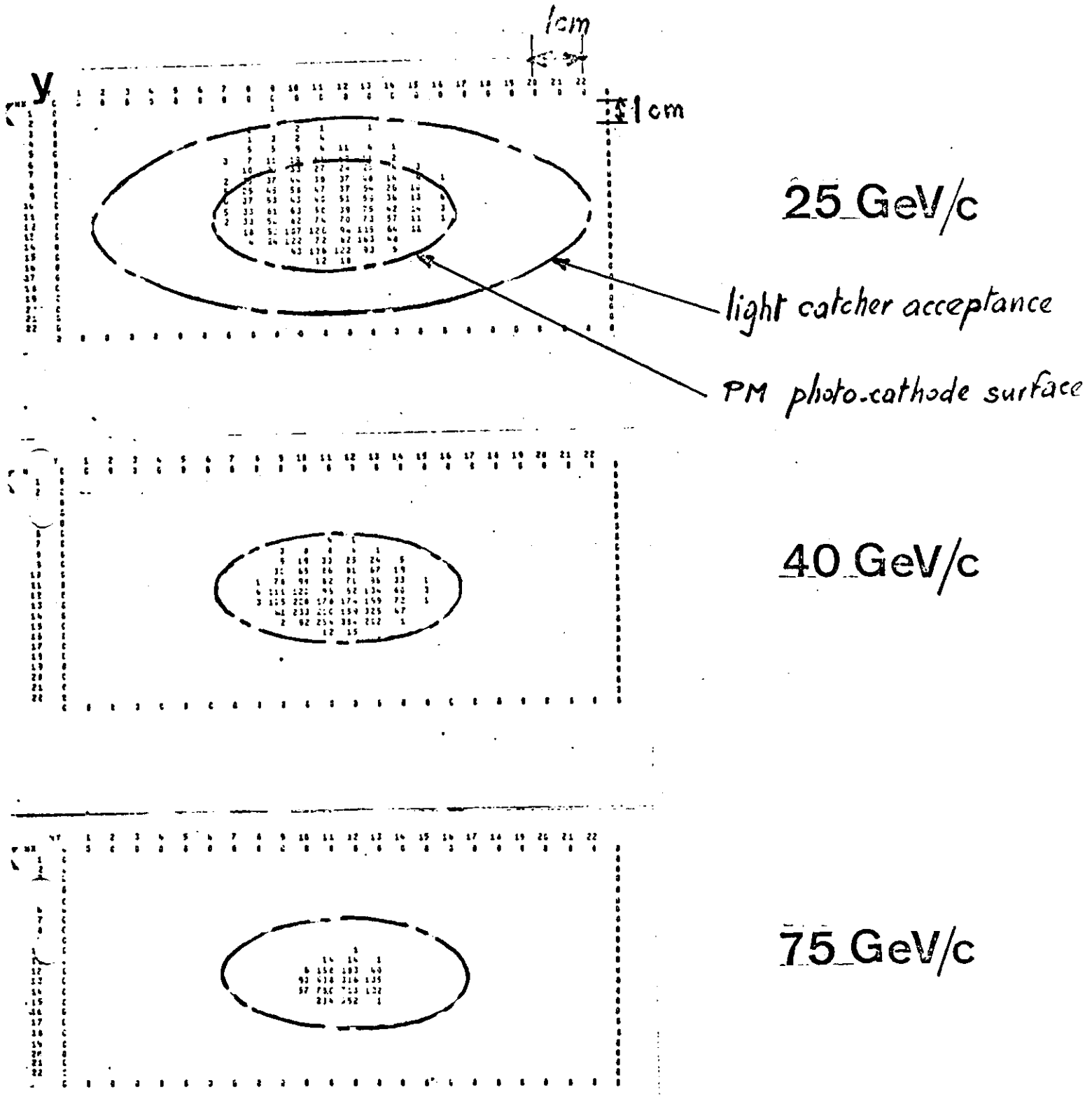

Photons impacts on the photocathode plane of TC1.

fig 1c

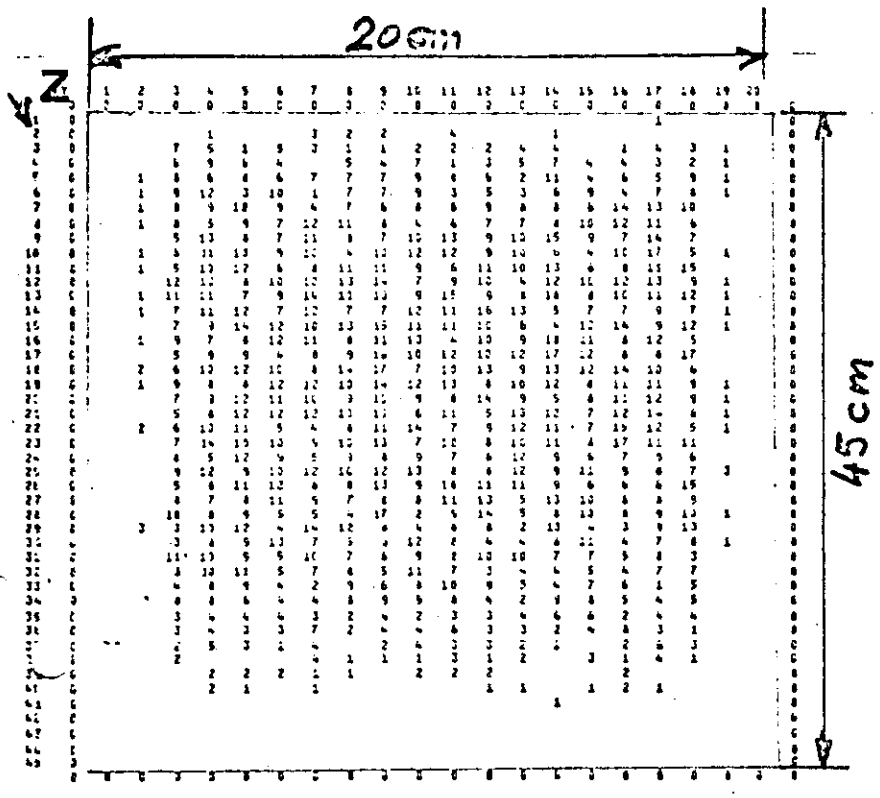

40 GeV/c

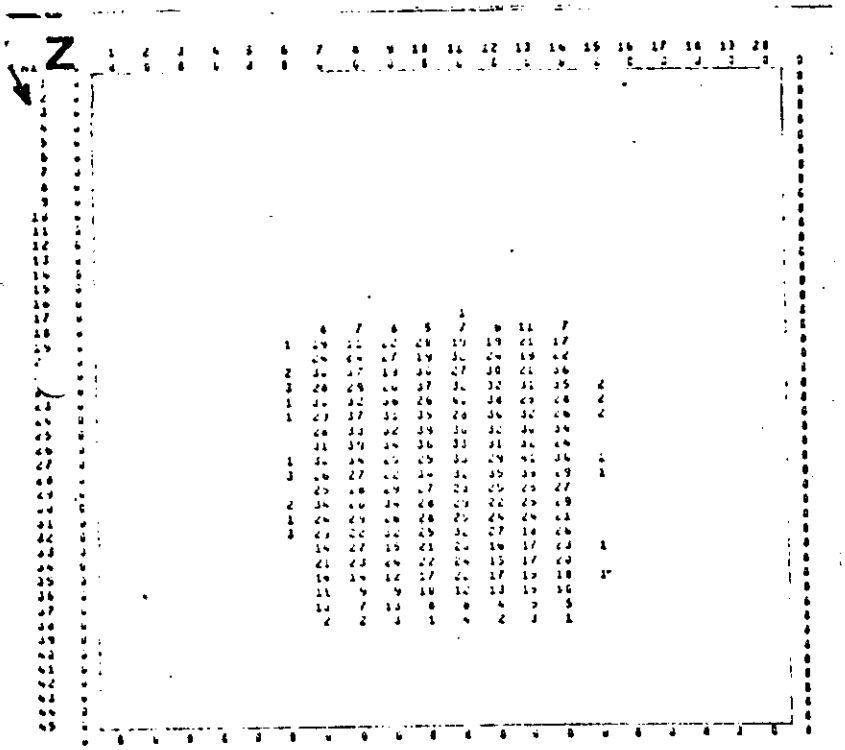

75 GeV/c

Charged particles impacts on entry face of TC2

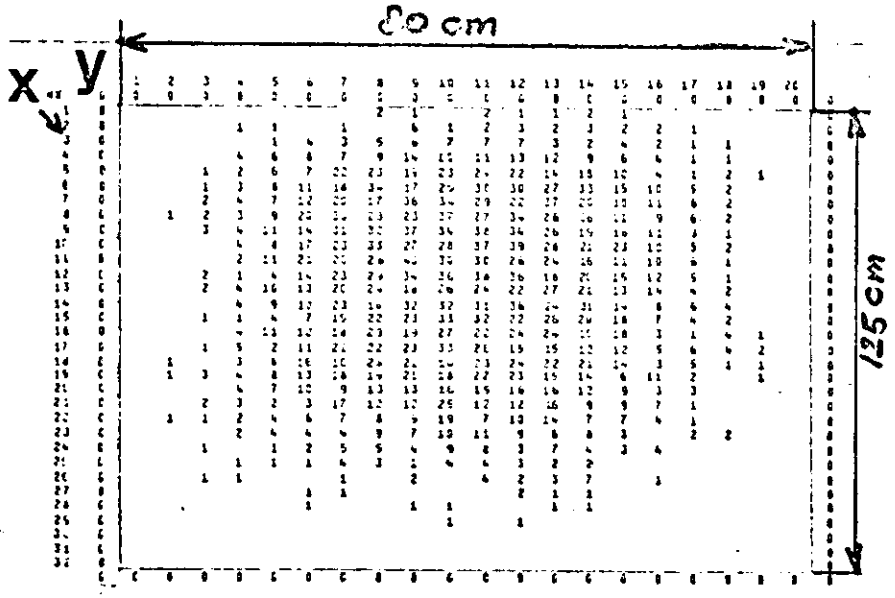

40 GeV/c

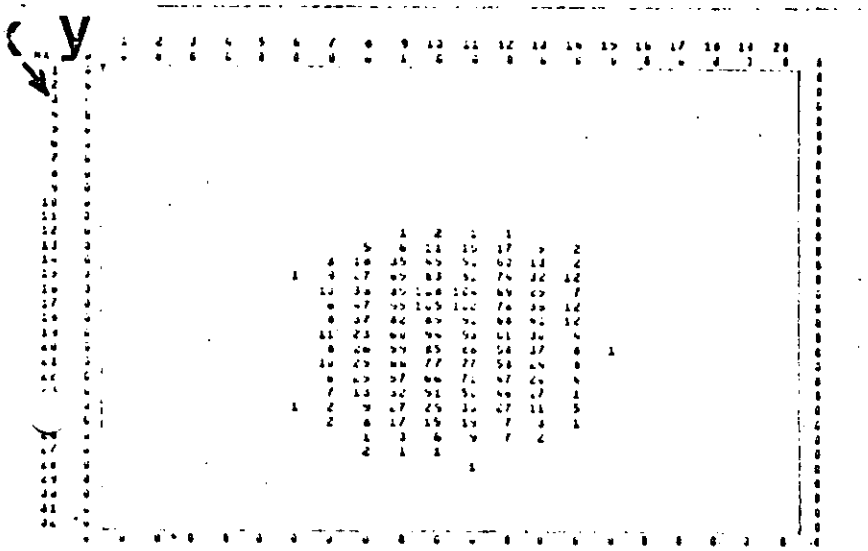

75 GeV/c

Photons impacts on the mirror of TC2

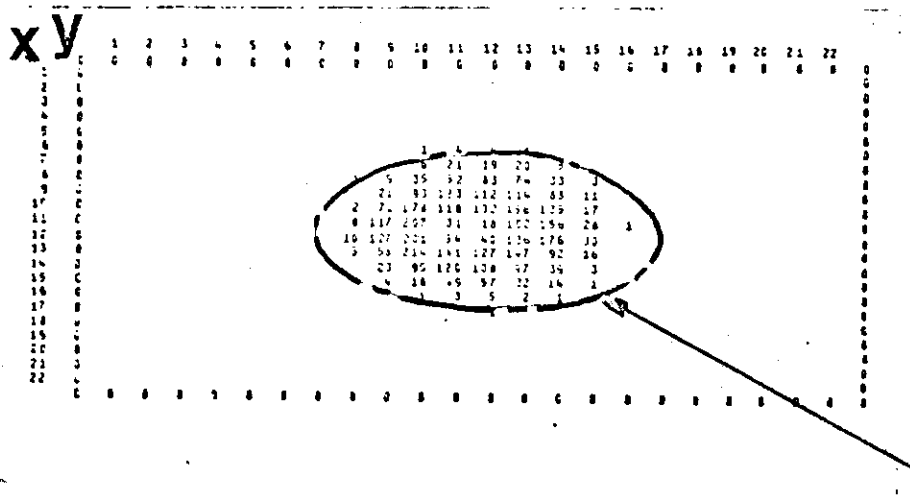

40 GeV/c

PM photo-cathode surface

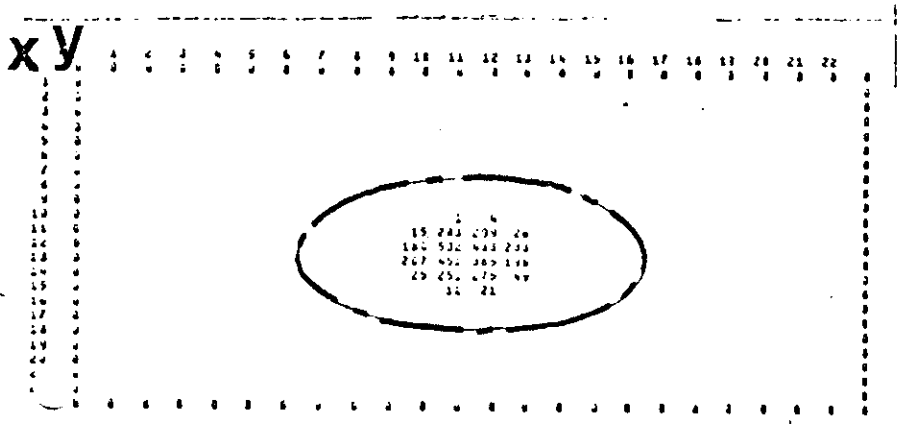

75 GeV/c

Photons impacts on the photo-cathode plane of TC_2

Fig 1.f

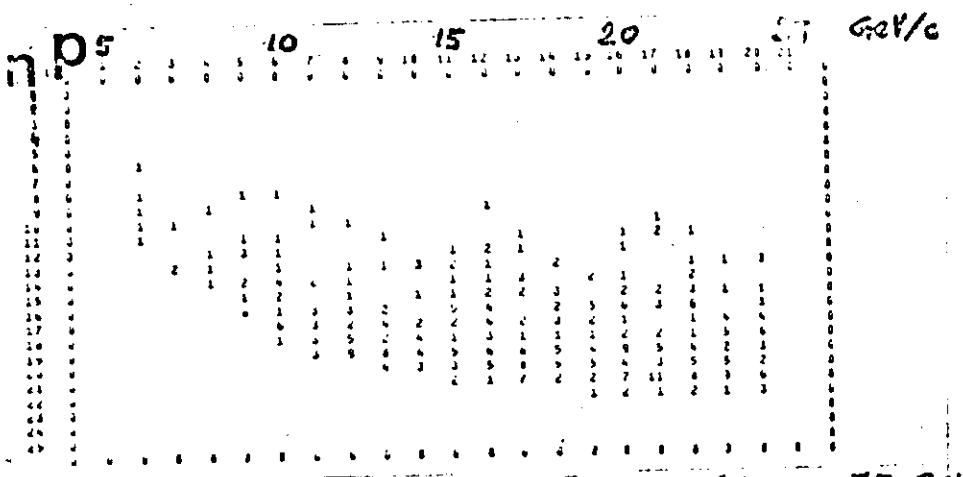

TC_1 at 25 GeV/c

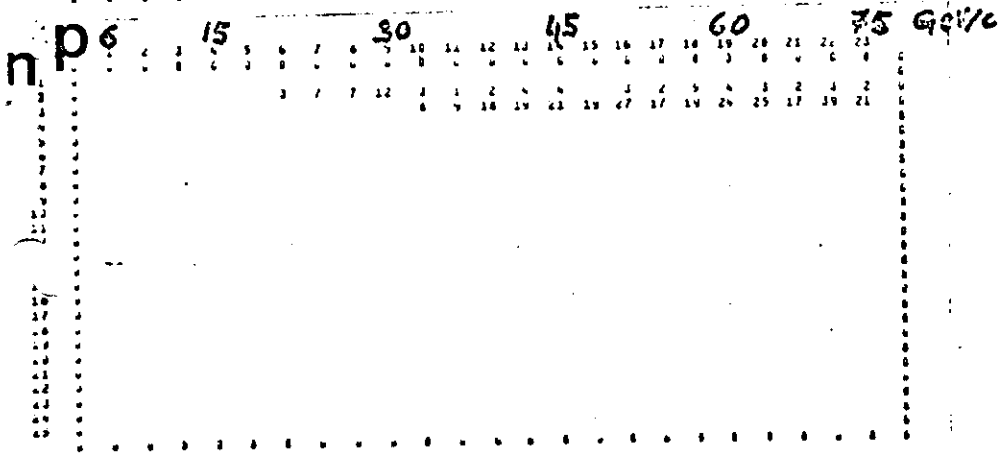

TC_1 at 75 GeV/c

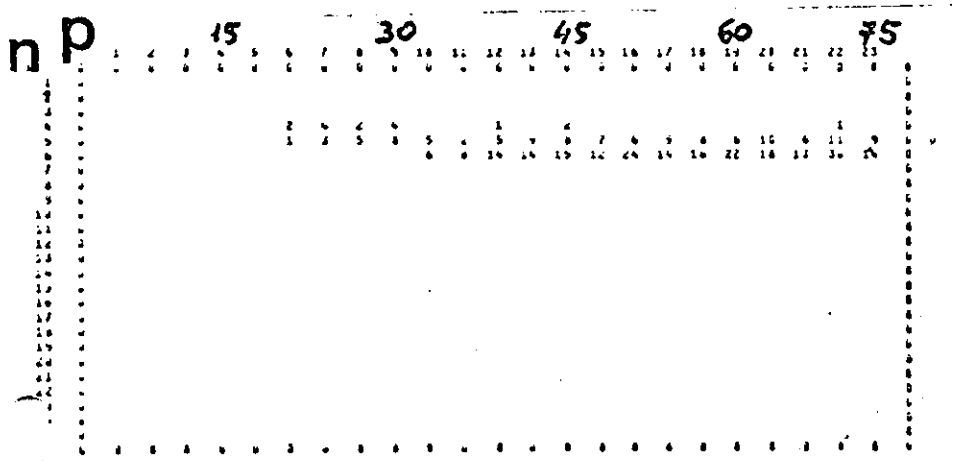

TC_2 at 75 GeV/c

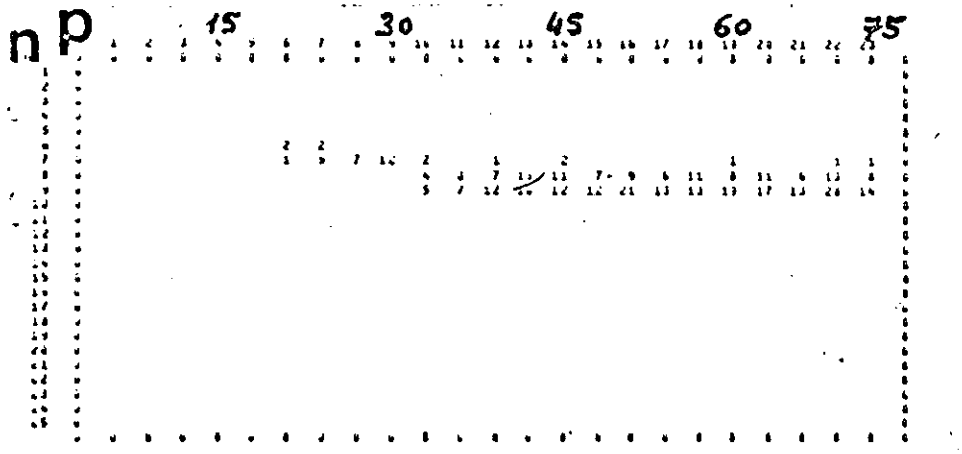

Total at 75 GeV/c

Inefficiencies for pions (10^{-n})

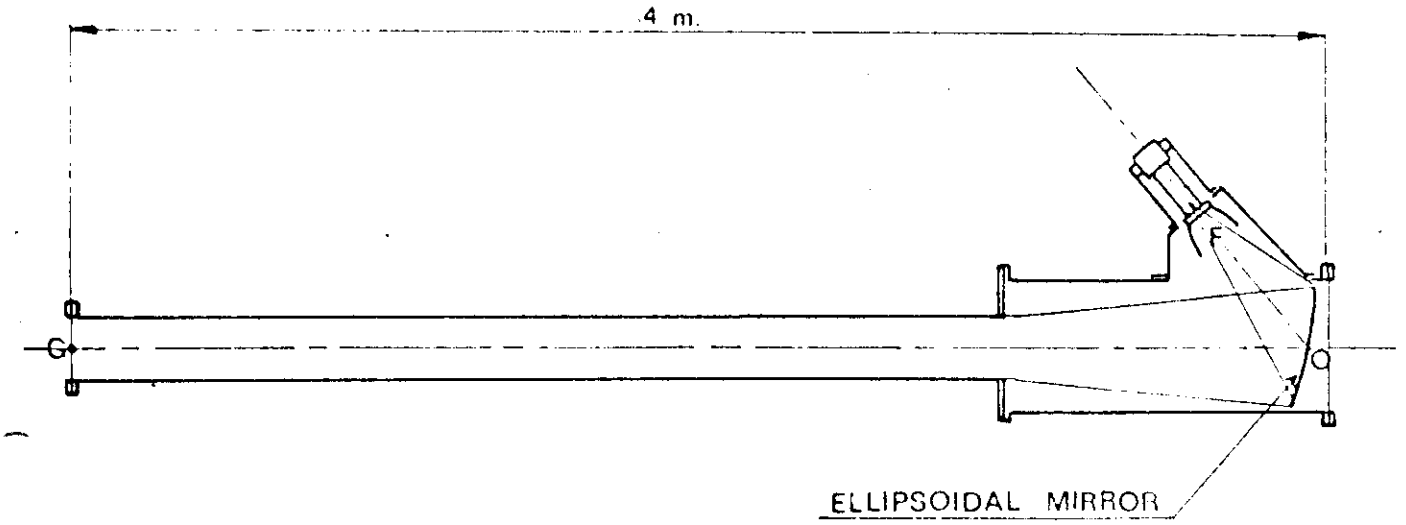
4 m.
F
G
O
ELLIPSOIDAL MIRROR

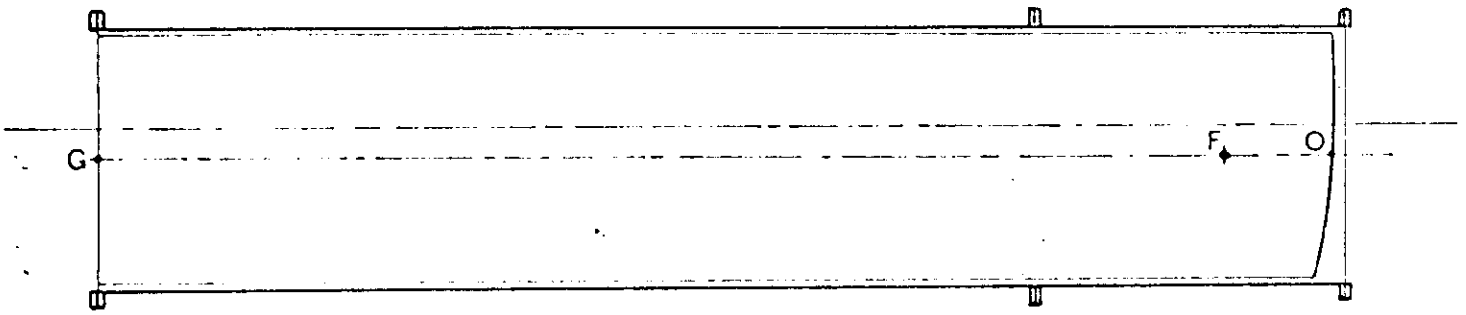
G
F
O

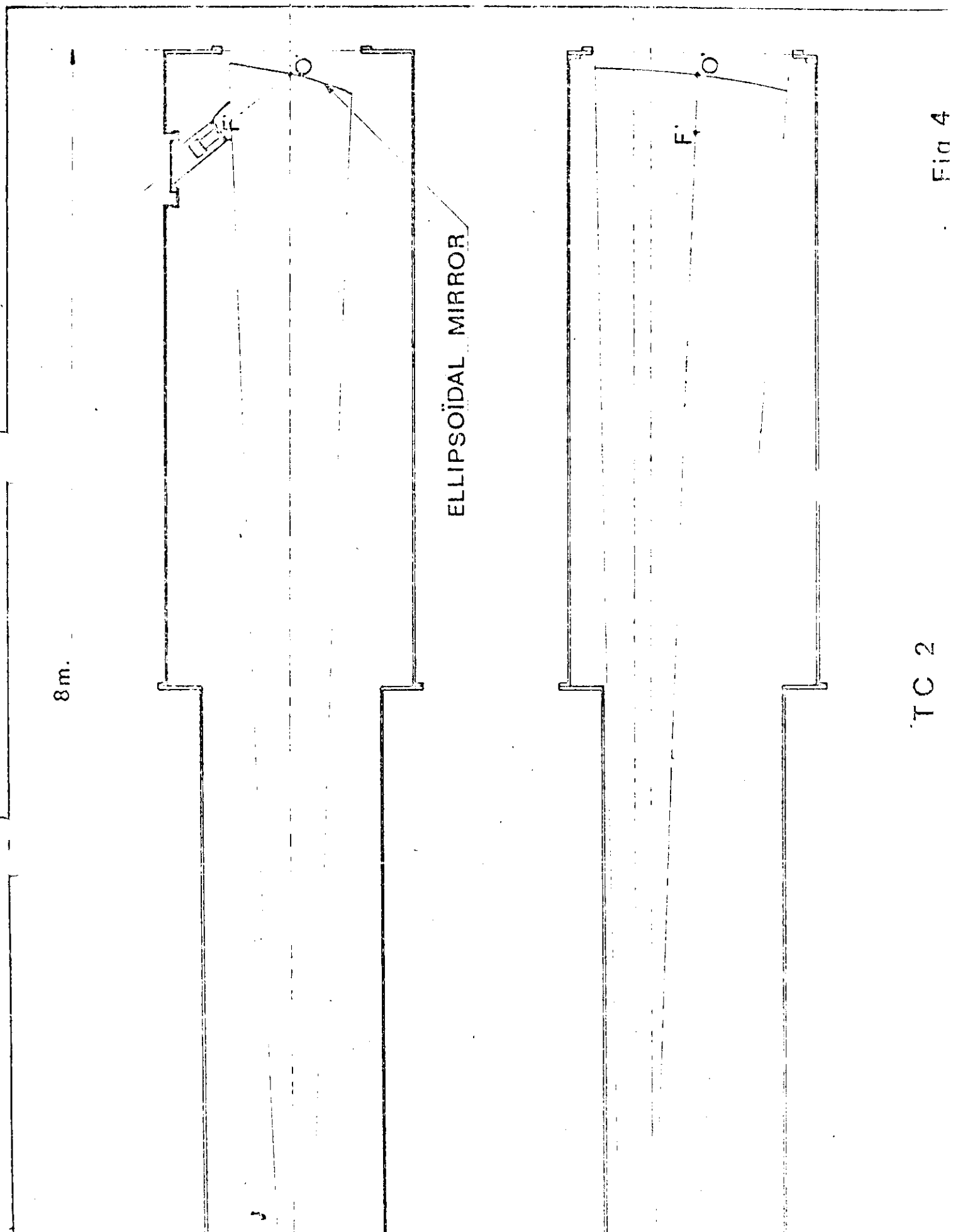

TC 2

Fig 4

APPENDIX II

PROPORTIONAL CHAMBERS

The low energy particles detection system is composed of 14 proportional chambers disposed symmetrically on each side of the target. The distance between the axis of the Goliath magnet and the first chamber is 100 mm. The useful area of each chamber is 1800 mm long, 740 mm high, and the total thickness is 112 mm. The distance between two chambers is 12cm. Each one, as seen on fig.1, is composed of 2 ground planes, 4 HV planes of horizontal wires (1970 wires) and 3 read-out planes (900 vertical wires, 370 horizontal wires and 590 wires which are 14°30' tilted).

The spacing of the bronze beryllium HV wires (50 μ diameter) is 1.5 mm, the tension applied is 100 gr. Nylon wires are added every 300 mm.

For the golden tungsten read-out wires (20 μ diameter) which are 2 mm spaced, we use a tension of 50 gr. These read-out wires are disposed in order to have the vertical wires plane closest to the beam axis, then we have the horizontal wires and the 14°30' tilted wires.

The gap between the HV plane and the read-out plane is 7 mm. The ground planes, as thin as possible, are in aluminized mylar and are used for the gas tightness (Figure 1).

The first chamber is now built up and electronic tests have started.

The high energy particle detection system PC 1 and PC 2 is made of two proportional chambers. The first one is 400 mm wide and 200 mm high, the second one is 900 mm wide and 650 mm high. Each of them has 3 read-out planes, the wires are 1 mm spaced.

The construction of those chambers which have classical dimensions

For the electronics associated to the wires we have the choice between the LETI MOS integrated circuit [1] and a homemade circuit (Figure 2). The final decision is to be taken before the end of February and depends on the yield of the industrial production. The price of both circuits is of the order 6 $ per wire.

Tests of both circuits have been made on 48 wires in a small chamber. By now the first big vertex chamber prototype has 500 wires equipped with the LETI circuit.

---

[1] Essais pratiques du circuit intégré M.O.S. "FILAS" LETI CENG, Grenoble, France (Preprint 1973).

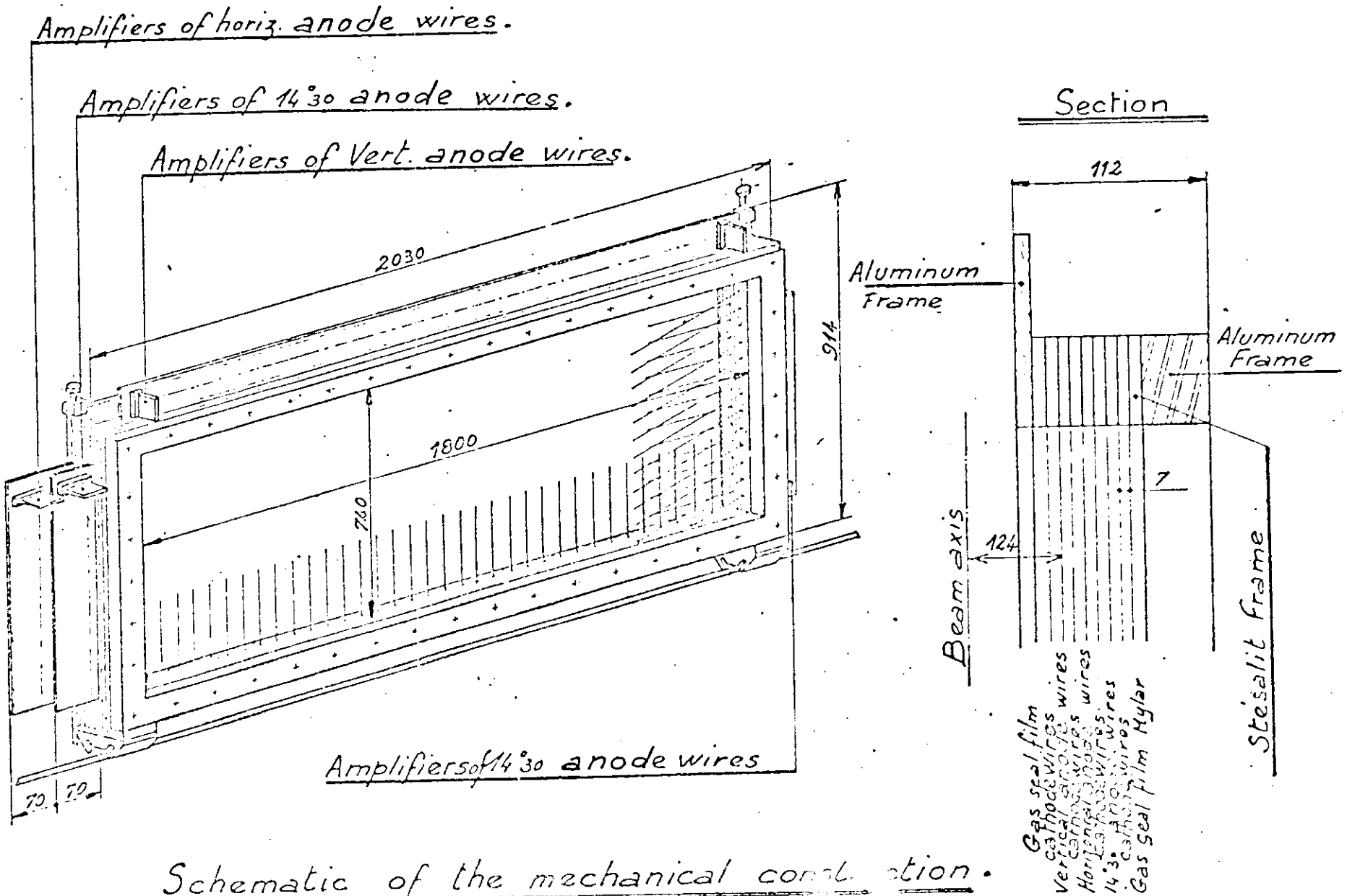

Schematic of the mechanical construction.

Fig 1

Dimensions in millimeters.

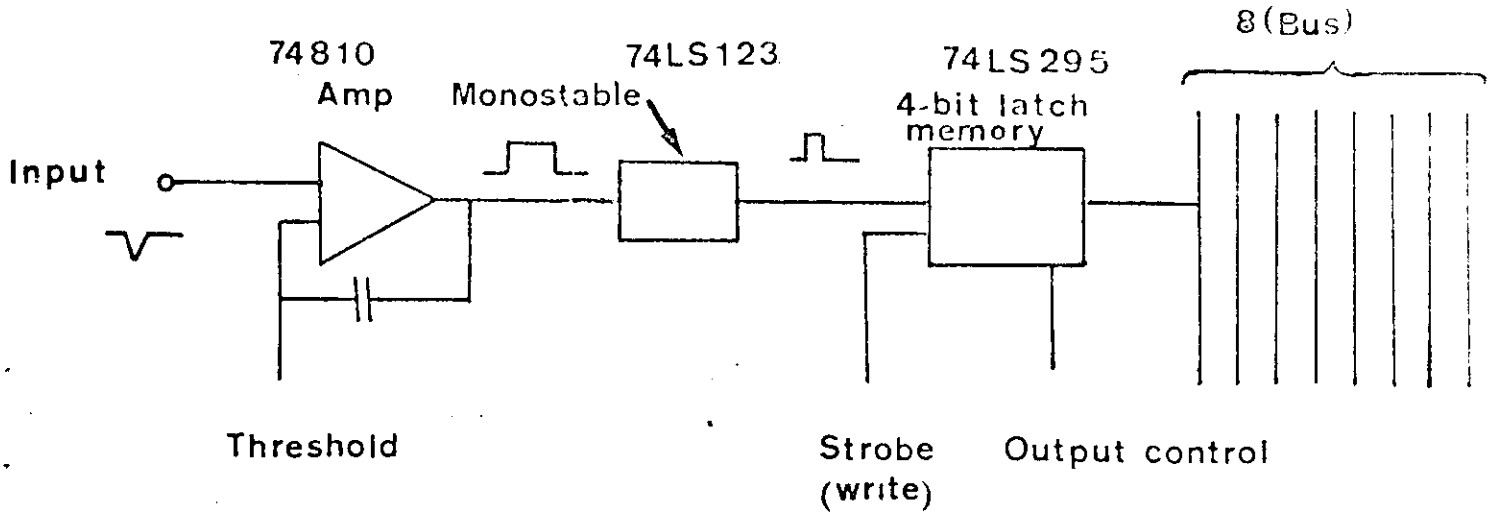

"LABORATORY" CIRCUIT

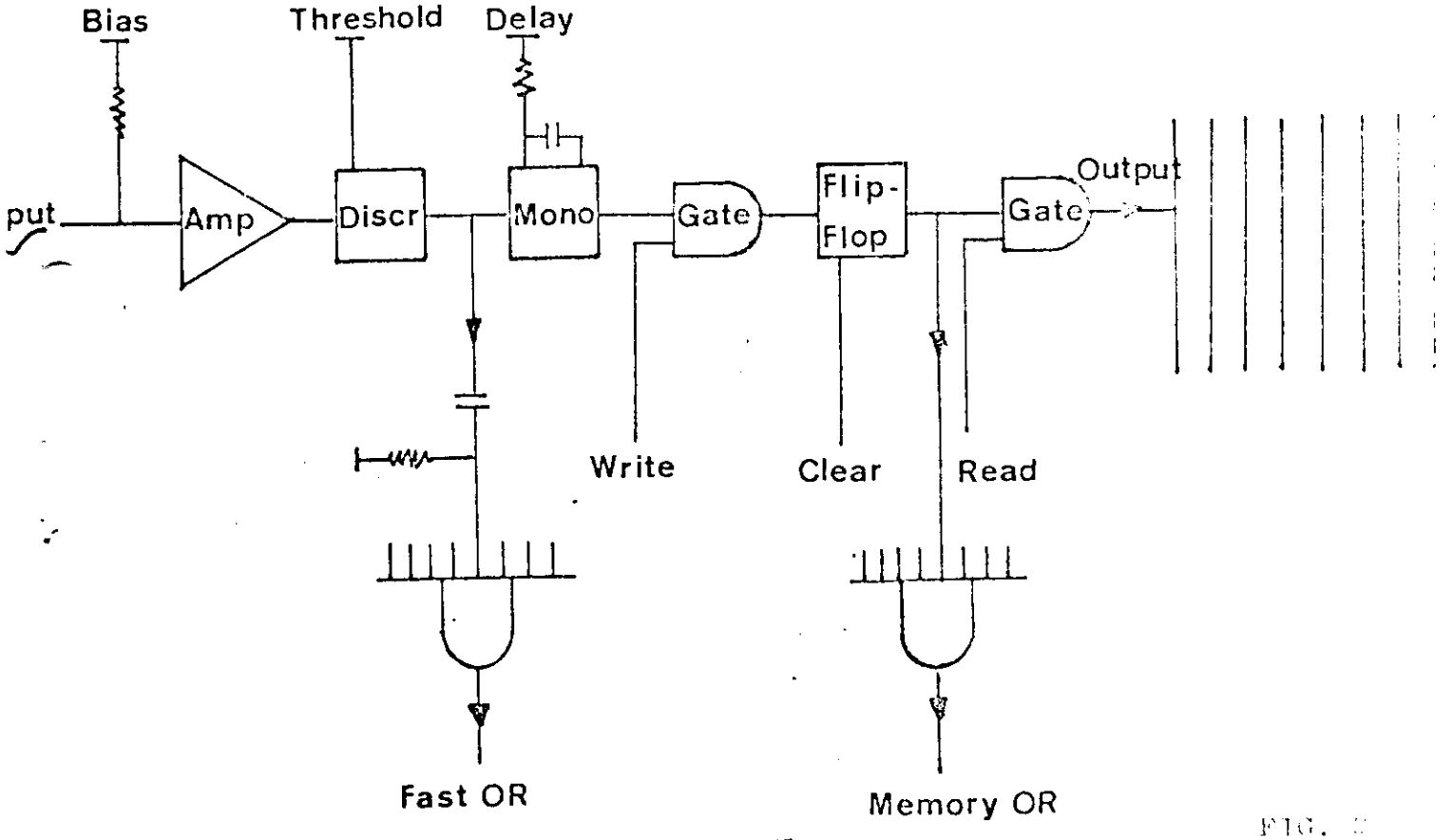

"LETI" CIRCUIT

FIG. 3